

Dimethyldihydropyrene–Dehydrobenzoannulene Hybrids: Studies in Aromaticity and Photoisomerization

David B. Kimball and Michael M. Haley*

Department of Chemistry and the Materials Science Institute, University of Oregon,
Eugene, Oregon 97403-1253

Reginald H. Mitchell,* Timothy R. Ward, and Subhajit Bandyopadhyay

Department of Chemistry, University of Victoria, P.O. Box 3065, Victoria, BC, Canada V8W3V6

Richard Vaughan Williams* and John R. Armantrout

Department of Chemistry, University of Idaho, P.O. Box 442343, Moscow, Idaho 83844-2343

haley@oregon.uoregon.edu; regmitch@uvic.ca; williams@neon.chem.uidaho.edu

Received July 11, 2002

The synthesis and study of dehydrobenzoannulene (DBA)–dimethyldihydropyrene (DDP) hybrids as models for the investigation of aromaticity in weakly diatropic systems is reported. Three new monofused DBA–DDP hybrids have been synthesized, and their NMR spectra are discussed with regard to quantifying the aromaticity remaining in multibenzene-fused DBAs. Nucleus-independent chemical shifts, determined at a series of locations for each compound, bond lengths, and ^1H and ^{13}C NMR chemical shifts were calculated and used to probe the aromaticity of these hybrids. Systems where more than one annulene/DBA is fused to the DDP core have also been obtained, and their potential use in photoinduced isomerization applications is discussed.

Introduction

In the area of materials research, few topics generate as much interest as finding next-generation electronics and photonics.¹ Two important fields in this broad spectrum² include nonlinear optical (NLO) susceptibility and photoinduced isomerization. The former has applications such as laser frequency multiplying and converting electronic signals to photonic information,³ while the latter is necessary for single-molecule-based memory devices.⁴ Key to both NLO susceptibility and photoisomerization is the ability to fine-tune the electronic characteristics of any suitable system. Although some

control can be achieved through logical substituent placement,^{3–5} often the electronic nature must be pre-imposed at the fundamental level. Since some of the most promising candidates for NLO and photoisomerization are highly conjugated sp- and sp²-based systems,⁵ issues of aromaticity and induced ring current are quite often a factor.

Aromaticity in large annulenes⁶ has been studied for many years, using a variety of macrocycles as model structures.⁷ The addition of sp carbon atoms into conju-

(1) (a) *Conjugated Polymers and Related Materials: The Interconnection of Chemical and Electronic Structure*; Salaneck, W. R., Lundström, I., Ranby, B., Eds.; Oxford University Press: Oxford, 1993. (b) *Photonic and Optoelectronic Polymers*; Jenekhe, S. A., Wynne, K. J., Eds.; American Chemical Society: Washington, DC, 1995. (c) *Nonlinear Optics of Organic Molecules and Polymers*; Nalwa, H. S., Miyata, S., Eds.; CRC Press: New York, 1997. (d) *Electronic Materials: The Oligomer Approach*; Müllen, K., Wegner, G., Eds.; Wiley-VCH: Weinheim, Germany, 1998.

(2) Inter alia: (a) Norris, D. J.; Vlasov, Y. A. *Adv. Mater.* **2001**, *13*, 371–376. (b) De La Rue, R.; Smith, C. *Nature* **2000**, *408*, 653, 655–656. (c) Shen, Y.; Friend, C. S.; Jiang, Y.; Jakubczyk, D.; Swiatkiewicz, J.; Prasad, P. N. *J. Phys. Chem. B* **2000**, *104*, 7577–7587. (d) Hide, F.; Diaz-Garcia, M. A.; Schwartz, B. J.; Heeger, A. J. *Acc. Chem. Res.* **1997**, *30*, 430–436. (e) Pearson, D. L.; Jones, L., III; Schumm, J. S.; Tour, J. M. *Synth. Met.* **1997**, *84*, 303–306. (f) Mirkin, C. A.; Ratner, M. A. *Annu. Rev. Phys. Chem.* **1992**, *43*, 719–753. (g) Miller, J. S. *Adv. Mater.* **1990**, *2*, 495–497.

(3) Inter alia: (a) Molina, M. I. *Int. J. Mod. Phys. B* **2001**, *15*, 2409–2432. (b) Wolff, J. J.; Wortmann, R. *Adv. Phys. Org. Chem.* **1999**, *32*, 121–217. (c) Verbiest, T.; Houbrechts, S.; Kauranen, M.; Clays, K.; Persoons, A. *J. Mater. Chem.* **1997**, *7*, 2175–2189. (d) Reinhardt, B. A. *Trends Polym. Sci.* **1996**, *4*, 287–289.

(4) Inter alia: (a) Norsten, T. B.; Branda, N. R. *J. Am. Chem. Soc.* **2001**, *123*, 1784–1785. (b) Gobbi, L.; Seiler, P.; Diederich, F.; Gramlich, V. *Helv. Chim. Acta* **2000**, *83*, 1711–1723. (c) Feringa, B. L.; Huck, N. P. M.; Schoevaars, A. M. *Adv. Mater.* **1996**, *8*, 681–684. (d) Fissi, A.; Pieroni, O.; Balestreri, E.; Amato, C. *Macromolecules* **1996**, *29*, 4680–4685. (e) Ehmman, A.; Gompper, R.; Hartmann, H.; Müller, T. J. J.; Polborn, K.; Schültz, R. *Angew. Chem., Int. Ed. Engl.* **1994**, *33*, 572–575. (f) Feringa, B. L.; Jager, W. F.; de Lange, B. *Tetrahedron* **1993**, *49*, 8267–8310.

(5) Inter alia: (a) Sarkar, A.; Okada, S.; Matsuzawa, H.; Matsuda, H.; Nakanishi, H. *J. Mater. Chem.* **2000**, *10*, 819–828. (b) Segura, J. L.; Martin, N. *J. Mater. Chem.* **2000**, *10*, 2403–2435. (c) Coe, B. J. *Chem.–Eur. J.* **1999**, *5*, 2464–2471. (d) Samoc, M.; Samoc, A.; Luther-Davies, B. *Synth. Met.* **2000**, *109*, 79–83. (e) Cravino, A.; Moggio, I.; Dell'Erba, C.; Comoretto, D.; Cuniberti, C.; Dellepiane, G.; Giorgetti, E.; Grando, D.; Sottini, S. *Synth. Met.* **1999**, *102*, 943–944. (f) Spreiter, R.; Bosshard, C.; Knöpfle, G.; Günter, P.; Tykwinski, R. R.; Schreiber M.; Diederich, F. *J. Phys. Chem. B* **1998**, *102*, 29–32.

(6) (a) Staab, H. A.; Günther, P. *Chem. Ber.* **1977**, *110*, 619–630. (b) Garret, P. J. *Aromaticity*; Wiley: New York, 1986. (c) Balaban, A. T.; Banciu, M.; Ciorba, V. *Annulenes, Benzo-, Hetero-, Homo-Derivatives and their Valence Isomers*; CRC Press: Boca Raton, FL, 1987; Vols. 1–3. (d) Minkin, V. I.; Glukhovstev, M. N.; Simkin, B. Ya. *Aromaticity and Antiaromaticity*; Wiley: New York, 1994. (e) *Chem. Rev.* **2001**, *101* (5) (“Aromaticity” special issue).

(7) Mitchell, R. H. *Chem. Rev.* **2001**, *101*, 1301–1315 and references therein.

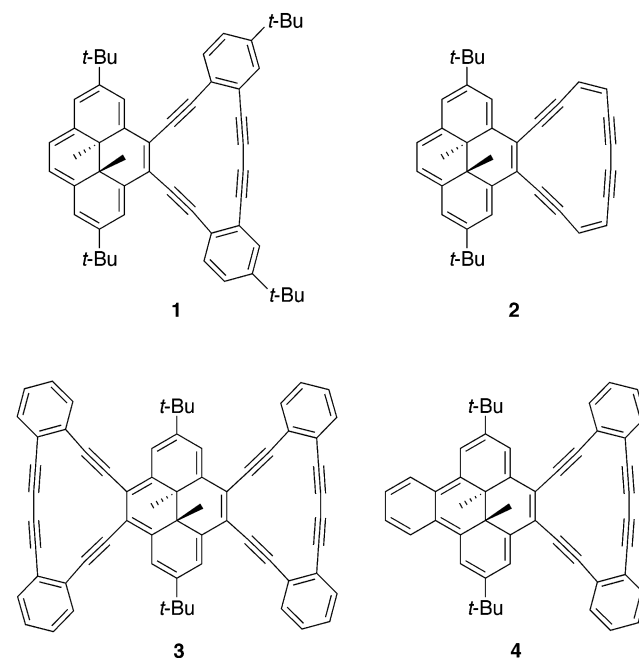
gated macrocycles, i.e., dehydroannulenes (DAs), can have surprising consequences. For more complex annulenes such as multiple-arene-fused systems and extended acetylenic macrocycles, i.e., dehydrobenzoannulenes (DBAs), traditional theories of aromaticity and ring currents are insufficient to predict or explain electronic character. Combining our studies⁸ with those of Vollhardt,⁹ Youngs,¹⁰ Bunz,¹¹ and others,¹² we have found the weak diatropicity in these large systems to be a much debated and challenging topic of research.

Two methods based on new experimental and theoretical models have emerged for the quantification of aromaticity. Mitchell has shown that dimethyldihydropyrene (DDP) can be used as a probe for the bond-fixing ability of arenes, which can be directly related to the diatropicity of a specific ring system.^{7,13} Fusing an aromatic moiety to the DDP core causes a reduction in the ring current of the pyrene, which is observable as a change in the chemical shift of the aromatic protons ($\delta \approx 8.5\text{--}9$ ppm) and the internal methyl protons ($\delta \approx -3.5$ to -4.5 ppm). Any deviation in the DDP ring current will alter the shielding/deshielding of the DDP protons; thus, comparing these resonance shifts with those induced by a fused benzene quantifies the aromaticity of the fused arene in question. To date, however, no DDP systems have been constructed which incorporate weakly diatropic molecules such as DBAs because of the difficulty in synthesizing larger annulene-fused DDP macrocycles.

Schleyer and co-workers developed a computational method to theoretically corroborate and understand experimental results regarding ring currents.¹⁴ They defined nucleus-independent chemical shifts (NICS) as the negative of the absolute shielding calculated using the Hartree–Fock (HF) gauge-invariant atomic orbital (GIAO) method, usually at the center of a ring system. By placing a ghost atom at the center of an aromatic or antiaromatic ring, one can observe the effects of diatropic or paratropic ring currents, respectively, manifested in the absolute shielding of the ghost atom. This powerful computational technique has been quickly adopted by

chemists¹⁵ and utilized, though not without some disagreement, to predict the aromaticity (or lack thereof) in DBAs.^{9,12}

In this paper, we present our efforts to assemble dehydroannulene-fused DDPs and thus determine the viability of using DDP to probe the aromatic character of DAs and DBAs.¹⁶ ¹H NMR studies and NICS calculations of the resultant hybrids (e.g., **1** and **2**) should allow for quantification of the aromaticity of the fused DAs and DBAs. In addition, it has been shown that the aromaticity of annulenes fused on opposing faces of a DDP can facilitate photoinduced isomerization to form the corresponding [2.2]metacyclophanediene.⁷ We hoped to use this knowledge to fine-tune the isomerization of the DDP core between the pyrene and the cyclophanediene forms; thus, we discuss our work to determine the viability of using DBA–DDP hybrids (e.g., **3** and **4**) for photoswitching applications.



(8) (a) Kimball, D. B.; Wan, W. B.; Haley, M. M. *Tetrahedron Lett.* **1998**, *39*, 6795–6798. (b) Bell, M. L.; Chiechi, R. C.; Johnson, C. A.; Kimball, D. B.; Matzger, A. J.; Wan, W. B.; Weakley, T. J. R.; Haley, M. M. *Tetrahedron* **2001**, *57*, 3507–3520. (c) Wan, W. B.; Chiechi, R. C.; Weakley, T. J. R.; Haley, M. M. *Eur. J. Org. Chem.* **2001**, 3485–3490. (d) Boydston, A. J.; Haley, M. M. *Org. Lett.* **2001**, *3*, 3599–3601. (e) Boydston, A. J.; Haley, M. M.; Williams, R. V.; Armantrout, J. R. *J. Org. Chem.* **2002**, *67*, 8812–8819.

(9) Matzger, A. J.; Vollhardt, K. P. C. *Tetrahedron Lett.* **1998**, *39*, 6791–6794.

(10) Zhang, D.; Tessier, C. A.; Youngs, W. J. *Chem. Mater.* **1999**, *11*, 3050–3057.

(11) (a) Laskoski, M.; Smith, M. D.; Morton, J. G. M.; Bunz, U. H. F. *J. Org. Chem.* **2001**, *66*, 5174–5181. (b) Laskoski, M.; Steffen, W.; Smith, M. D.; Bunz, U. H. F. *Chem. Commun.* **2001**, 691–692. (c) Bunz, U. H. F.; Roidl, G.; Altmann, M.; Enkelmann, V.; Shimizu, K. D. *J. Am. Chem. Soc.* **1999**, *121*, 10719–10726.

(12) (a) Jusélius, J.; Sundholm, D. *Phys. Chem. Chem. Phys.* **2001**, *3*, 2433–2437. (b) Alkorta, I.; Rozas, I.; Elguero, J. *Tetrahedron* **2001**, *57*, 6043–6049.

(13) (a) Mitchell, R. H.; Iyer, V. S.; Khalifa, N.; Mahadevan, R.; Venugopalan, S.; Weerawarna, S. A.; Zhou, P. *J. Am. Chem. Soc.* **1995**, *117*, 1514–1532. (b) Mitchell, R. H.; Iyer, V. S. *J. Am. Chem. Soc.* **1996**, *118*, 2903–2906. (c) Mitchell, R. H.; Chen, Y. *Tetrahedron Lett.* **1996**, *37*, 5239–5242.

(14) (a) Schleyer, P. v. R.; Maerker, C.; Dransfeld, A.; Jiao, H.; van Eikema Hommes, N. J. R. *J. Am. Chem. Soc.* **1996**, *118*, 6317–6318. (b) Cyranski, M.; Krygowski, T.; Wisiorowski, M.; Hommes, N.; Schleyer, P. v. R. *Angew. Chem., Int. Ed.* **1998**, *37*, 177–180.

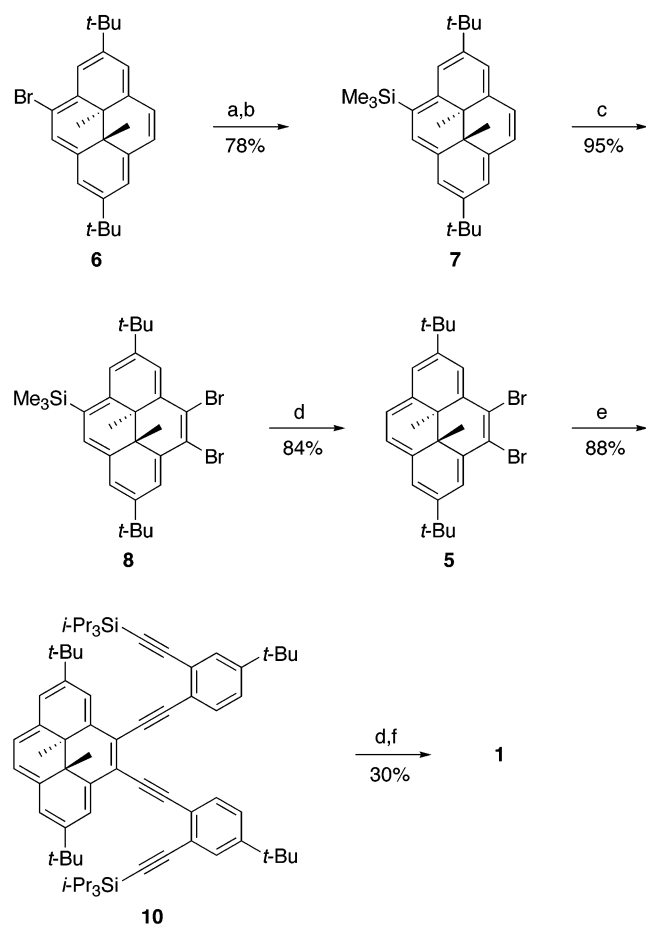
Results and Discussion

Monofused DDPs as Aromaticity Probes. The synthetic strategy for monoannulated DDP hybrids is based on dibromo-DDP **5** (Scheme 1). Although the correct regioisomeric dibromide could not be obtained by direct halogenation of the DDP, this key starting material was prepared in four steps from monobromo-DDP **6**.¹⁷ Lithium–halogen exchange followed by addition of

(15) Inter alia: (a) Gomes, J. A. N. F.; Mallion, R. B. *Chem. Rev.* **2001**, *101*, 1349–1383. (b) Cyranski, M. K.; Krygowski, T. M.; Katritzky, A. R.; Schleyer, P. v. R. *J. Org. Chem.* **2002**, *67*, 1333–1338. (c) Schleyer, P. v. R.; Manoharan, M.; Wang, Z.-X.; Kiran, B.; Jiao, H.; Puchta, R.; van Eikema Hommes, N. J. R. *Org. Lett.* **2001**, *3*, 2465–2468. (d) Stahl, F.; Moran, D.; Schleyer, P. v. R.; Prall, M.; Schreiner, P. R. *J. Org. Chem.* **2002**, *67*, 1453–1461. (e) West, R.; Buffy, J. J.; Haaf, M.; Müller, T.; Gehrhuis, B.; Lappert, M. F.; Apeloig, Y. *J. Am. Chem. Soc.* **1998**, *120*, 1639–1640. (f) Chen, Z.; Jiao, H.; Hirsch, A.; Thiel, W. *J. Org. Chem.* **2001**, *66*, 3380–3383. (g) Havenith, R. W. A.; van Lenthe, J. H.; Dijkstra, F.; Jenneskens, L. W. *J. Phys. Chem. A* **2001**, *105*, 3838–3845.

(16) Kimball, D. B.; Haley, M. M.; Mitchell, R. H.; Ward, T. R. *Org. Lett.* **2001**, *3*, 1709–1711.

(17) Mitchell, R. H.; Ward, T. R. *Tetrahedron* **2001**, *57*, 3689–3695.

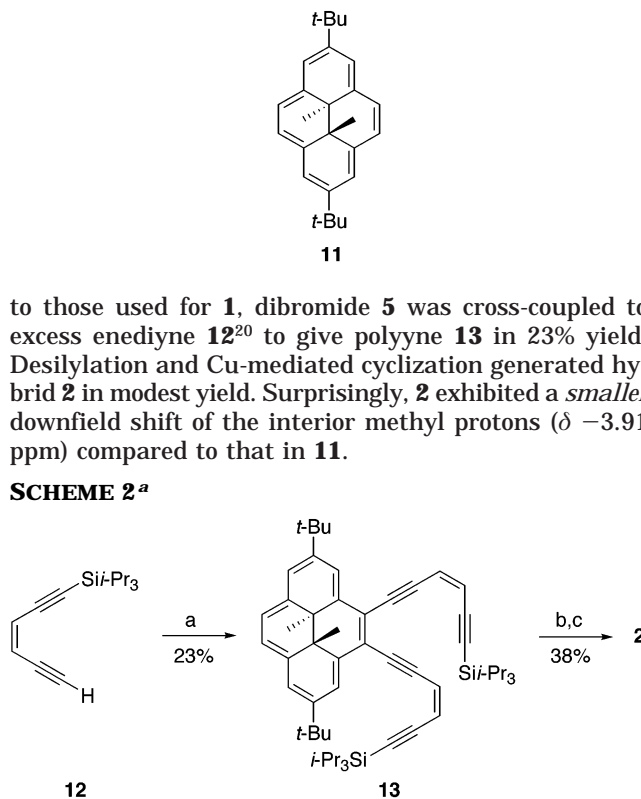
SCHEME 1^a

^a Reagents and conditions: (a) BuLi, THF; (b) Me₃SiCl; (c) NBS, DMF, CH₂Cl₂; (d) Bu₄NF, MeOH, THF; (e) **9**, PdCl₂(PPh₃)₂, Pd(PPh₃)₄, CuI, DMF, Et₃N, 100 °C; (f) CuCl, pyridine, MeOH, THF.

Me₃SiCl gave compound **7**, which now has three of the DDP rings sterically blocked to bromination. Dihalogenation on the remaining open face of **7** with NBS provided compound **8**. Subsequent removal of the silyl group with fluoride ion gave **5** in 62% yield from **6**. Cross-coupling dibromide **5** with excess 4-*tert*-butyl-1-ethynyl-2-(triisopropylsilyl)ethynylbenzene (**9**), prepared in two steps from 4-*tert*-butyl-1-iodo-2-(triisopropylsilyl)ethynylbenzene,¹⁸ afforded polyynyl **10** in 88% yield. Although a number of procedures were available, we found that inclusion of DMF as cosolvent¹⁹ was necessary for cross-couplings with the bromo-DDPs to proceed in very good yields. Desilylation and cyclization using CuCl in pyridine/THF furnished the desired mono[14]DBA-DDP hybrid **1** in 26% overall yield from **5**.

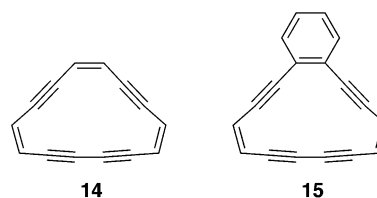
¹H NMR analysis of **1** showed a small but distinct downfield shift of the DDP methyl resonances (δ -3.71 ppm) when compared with that of the parent di-*tert*-butyl-DDP **11** (δ -4.06 ppm), a result that would be consistent with an aromatic ring fused to the DDP core. Nevertheless, the ring currents in DBAs are known to be very weak; thus, we decided to increase the aromaticity of the dehydro[14]annulene by removal of the two

fused benzenes.^{8d,e} The resulting hybrid **2** was synthesized as shown in Scheme 2. Using conditions analogous



^a Reagents and conditions: (a) **5**, PdCl₂(PPh₃)₂, Pd(PPh₃)₄, CuI, DMF, Et₃N, 100 °C; (b) Bu₄NF, MeOH, THF; (c) CuCl, pyridine, MeOH, THF.

Whereas the DDP methyls indicate little or no ring current of the fused [14]annulene, the alkene protons of the latter suggest a different story. We^{8d,e} and others^{11a,b} have shown that the protons on octadehydro[14]annulene (**14**), although not as accurate as the DDP skeleton, are a very good, qualitative indicator of the aromaticity of a fused-ring system. As shown in Table 1, the alkene protons in **2** are in approximately the same region as those in **15**, both of which are significantly upfield from

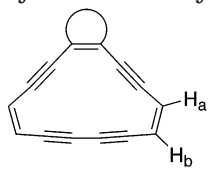


those in **14**. This suggests that the ring current in the DDP core is about the same as that in a benzene ring. Interestingly, all three systems show marked downfield shifts (ca. 0.6–1.8 ppm) of their respective alkene protons upon cyclization of their polyynyl precursors, indicating the presence of a discernible diatropic ring current.

To examine the effect on the DDP ring current from the 14-membered cycle, we prepared hybrid **16**, where the bridging alkenes were replaced by alkane units (Scheme 3). Diyne **17**²¹ was coupled to **5** to give polyynyl

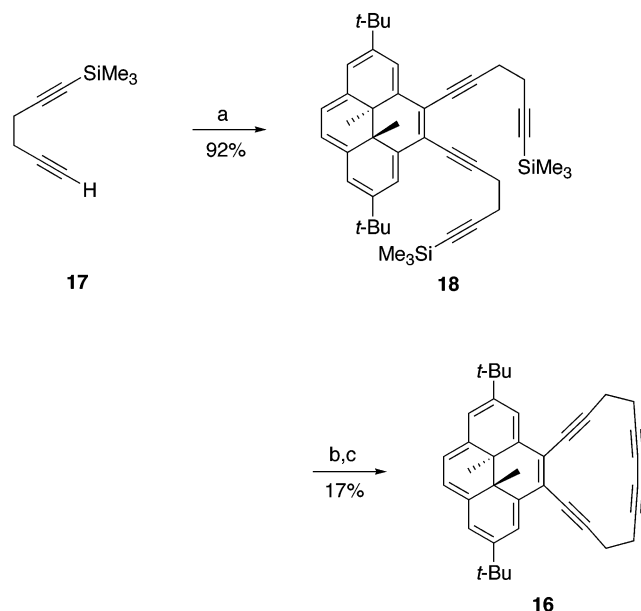
(18) Wan, W. B.; Haley, M. M. *J. Org. Chem.* **2001**, *66*, 3893–3901.
 (19) Sjögren, M.; Hansson, S.; Norrby, P.-O.; Akermark, B.; Cucciolito, M. E.; Vitagliano, A. *Organometallics* **1992**, *11*, 3954–3964.

(20) Lu, Y.-F.; Harwig, C. W.; Fallis, A. G. *J. Org. Chem.* **1993**, *58*, 4202–4204.

TABLE 1. Chemical Shifts (ppm) of the Alkene Protons in Precyclized and Cyclized Octadecyhydro[14]annulenes^a


| proton | no fusion ^b | | benzo-fused ^b | | DDP-fused | |
|----------------|------------------------|-----------|--------------------------|-----------|-----------|----------|
| | pre- 14 | 14 | pre- 15 | 15 | 13 | 2 |
| H _a | 6.05 | 7.92 | 6.17 | 7.41 | 6.41 | 7.66 |
| H _b | 5.90 | 7.39 | 5.94 | 6.73 | 6.00 | 6.61 |

^a In CD₂Cl₂. ^b Reference 8e.

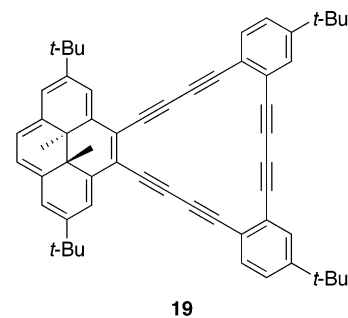
SCHEME 3^a

^a Reagents and conditions: (a) **5**, PdCl₂(PPh₃)₂, Pd(PPh₃)₄, CuI, DMF, Et₃N, 100 °C; (b) K₂CO₃, MeOH, THF; (c) CuCl, pyridine, MeOH, THF.

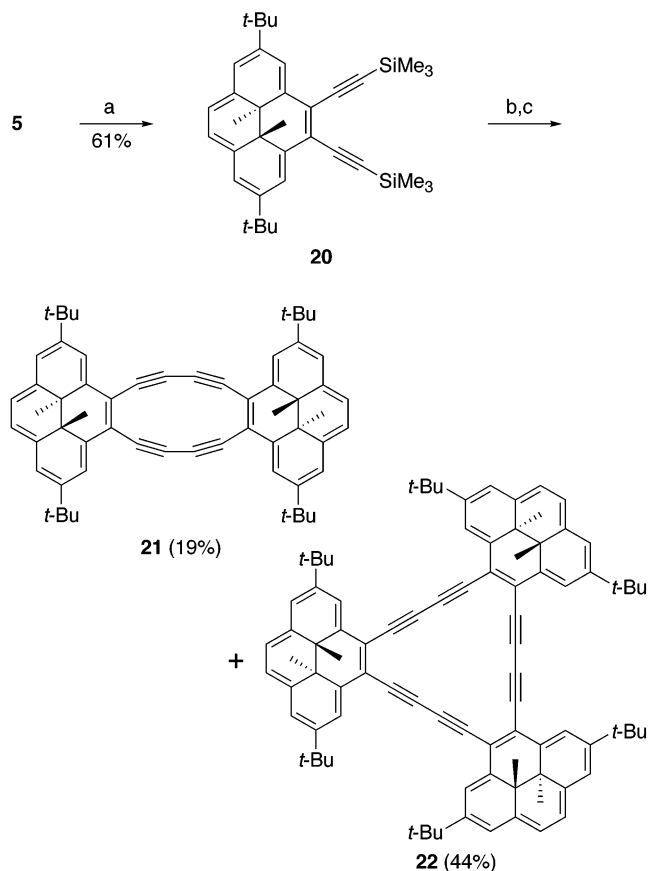
18 in 92% yield. Desilylation and Cu-mediated cyclization gave **16** in low yield. In this case, the chemical shift of the methyl protons of **16** (δ –3.77 ppm) was essentially the same as found in **1** (δ –3.71 ppm). These results again suggest little or no diatropicity for the octadecyhydro[14]-annulene nucleus.

For all monofused hybrids studied, the one that shows the least weakening of the DDP ring current is hybrid **2**, which is exactly the reverse of what we expected. These curious findings might be attributable to either the anisotropy of the triple bonds or geometric deformation. X-ray crystal analysis of related tribenzooctadecyhydro[14]annulene shows significant bending of the triple bonds.²² This could result in σ inductive effects due to strain or pronounced π donation from the bent acetylenes. To test whether this was a factor in our systems, we attempted the synthesis of mono[18]DBA–DDP **19**. Since [18]DBAs have been shown to be essentially planar and

free of strain,²³ this would give a better indication of whether the DDP core could be used to test weakly diatropic systems.



Unlike previous [18]DBA syntheses, the sluggish reactivity of **5** necessitated use of sequential acetylene–haloarene and acetylene–acetylene cross-couplings to install the initial diyne linkages. Combining **5** with excess (trimethylsilyl)acetylene afforded diethynyl-DDP **20** in 61% yield (Scheme 4). After desilylation, the terminal alkynes were subjected to 1-bromoethynyl-2-(triisopropylsilyl)ethynylbenzene^{8b} using a modified Cadiot–Chodkiewicz reaction.²⁴ Surprisingly, none of the expected α,ω -hexayne was obtained; instead, a 7:3 mixture of bis(DDP)–[12]annulene **21** and tris(DDP)–[18]annulene **22** was obtained in 63% yield. Repetition

SCHEME 4^a

(21) Hillard, R. L., III; Vollhardt, K. P. C. *J. Am. Chem. Soc.* **1977**, *99*, 4058–4069.

(22) Baldwin, K. P.; Matzger, A. J.; Scheiman, D. A.; Tessier, C. A.; Vollhardt, K. P. C.; Youngs, W. J. *Synlett* **1995**, 1215–1218.

^a Reagents and conditions: (a) Me₃SiC≡CH, PdCl₂(PPh₃)₂, Pd(PPh₃)₄, CuI, DMF, Et₃N, 100 °C; (b) Bu₄NF, THF, MeOH; (c) 1-(bromoethynyl)-2-(triisopropylsilyl)ethynylbenzene, Pd(dba)₂, CuI, LiI, DMSO, 1,2,2,6,6-pentamethylpiperidine.

TABLE 2. Chemical Shifts (ppm) of Selected Arene Protons in Precyclized and Cyclized DBA–DDP Hybrids^a

| proton ^b | 10 | 1 | 13 | 2 | 18 | 16 | 20 | 21 | 22 |
|---------------------|------|------|------|------|------|------|------|------|------|
| H9/14 | 8.46 | 8.59 | 8.46 | 8.69 | 8.46 | 8.46 | 8.47 | 8.33 | 8.57 |
| H11/12 | 8.38 | 8.48 | 8.39 | 8.59 | 8.38 | 8.38 | 8.39 | 8.27 | 8.48 |

^a In CDCl₃. ^b Proton numbering corresponds to the DDP assignments in Figure 2 and Table S3.

of this experiment with other conditions for acetylene–bromoacetylene heterocoupling afforded the same products in slightly different ratios. It is interesting to note, however, that tris(DDP)–[18]annulene **22** showed a downfield shift in methyl proton resonances compared to diethynyl-DDP **20** ($\delta(\text{Me}) -3.56$ for **22** and -3.76 for **20**).

In addition to the methyl resonances, the DDP arene protons can be used to estimate the aromaticity of a fused ring system. The chemical shift values of H9/14 and H11/12 for the five hybrids and their uncyclized precursors are given in Table 2. This should be a more valid comparison for our systems since each of the molecules contains the same 4,5-diethynyl-DDP moiety, yet the arene protons in question are sufficiently remote that effects from conformational bias and anisotropy of the triple bonds should be negligible. Interestingly, the chemical shifts of the two resonances are within 0.01 ppm for all four precursors, and are the same as the values for H9/14 and H11/12 found in **16** (8.46 and 8.38, respectively). Introduction of a ring current in the annelated cycle shifts the resonances approximately 0.10 ppm downfield for **1** and **22**, and ca. 0.21 ppm downfield for **2**. Although a larger difference would be expected for the stronger diatropicity in **2**, the direction of the shift is in the wrong direction. Surprisingly, all of the NMR data suggest that the DDP core becomes *more aromatic* as the anticipated diatropicity of the fused 14-membered ring is increased, which is exactly opposite of what is expected.

Computational Studies. In an effort to explain these puzzling experimental data, we undertook a theoretical study of some octadehydro[14]annulenes (ODAs) and their analogues. The geometries for all compounds in this study were optimized using the B3LYP/6-31G* method as implemented in Jaguar 4.0²⁵ and, for compound **1** only, the Gaussian 98 suite of programs.²⁶ All optimized structures were confirmed to be minima through their calculated energy second derivatives. Gaussian 98²⁶ was used to calculate NICS values with the GIAO-HF method on the B3LYP/6-31G*-optimized geometry (GIAO-HF/6-31G**/B3LYP/6-31G*).

Schleyer et al. demonstrated that aromatic systems have negative NICS values (e.g., -11.5 for benzene) while antiaromatic systems have positive NICS values (e.g.,

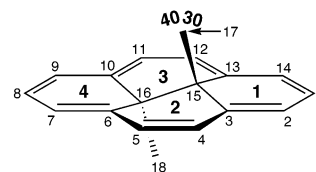
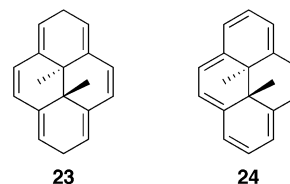


FIGURE 1. Numbering scheme and location of the NICS points for the DDP nucleus. NICS points are shown in bold type. Point 30 is 0.2 Å from C17 extended on a line joining C17 and C18. Point 40 is 0.2 Å from C17 on a line extending the C15–C17 bond.

+28.8 for cyclobutadiene) and nonaromatics have values near zero (e.g., -2.1 for cyclohexane).^{14a} NICS values are basis set dependent. Those reported above for benzene, cyclobutadiene, and cyclohexane and for the NICS studies reported herein were calculated using GIAO-HF/6-31G**/B3LYP/6-31G*.^{14a} NICS have been used to assess the aromaticities of individual rings in polycyclic aromatics and are also frequently calculated at points out of the ring plane(s) to avoid local anisotropies of the σ bonds.^{14,15c,27} Recently, we established that the B3LYP/6-31G*-calculated structures for three DDPs were in excellent agreement with the experimental X-ray structures.²⁸ Furthermore, confirming that the B3LYP/6-31G* method is appropriate for the investigation of DDPs, we found that ¹H (GIAO-HF/6-31G**/B3LYP/6-31G*) and ¹³C (scaled²⁹ from GIAO-B3LYP/6-31G**/B3LYP/6-31G*) NMR chemical shifts calculated at the optimized B3LYP/6-31G* geometries for 12 DDPs closely matched the corresponding experimental data.²⁸ Using these methods, we verified that NICS not only allow for a qualitative detection of aromaticity, but also provide exact correlation with an experimental scale of aromaticity derived for a large series of DDPs.²⁸ The simple arithmetic average of NICS (NICS_{AV}) calculated at the centers of the four six-membered rings (points 1–4, Figure 1) of the DDP nuclei gave the most reliable ordering of aromaticities of the DDP nucleus.²⁸ In addition, NICS values determined at the out-of-plane points 30 and 40 (Figure 1) also effectively ordered the aromaticities in the majority of cases studied.²⁸

We defined the relative aromaticity (RA) of the DDP nucleus in terms of the nonaromatic model **23** and the DDP (**n**) under investigation referenced to the *fully* aromatic parent DDP (**24**) by means of eqs 1–3.²⁸



Similarly, the RA of the ODA nucleus can be defined using the nonaromatic model **25**³⁰ and the appropriate

(23) Pak, J. J.; Weakley, T. J. R.; Haley, M. M. *J. Am. Chem. Soc.* **1999**, *121*, 8182–8192.

(24) Cai, C.; Vasella, A. *Helv. Chim. Acta* **1995**, *78*, 2053–2064.

(25) Jaguar 4.0, Schrödinger, Inc., Portland, OR, 1991–2000.

(26) Gaussian 98, Revision A.9, Frisch, M. J.; Trucks, G. W.; Schlegel, H. B.; Scuseria, G. E.; Robb, M. A.; Cheeseman, J. R.; Zakrzewski, V. G.; Montgomery, J. A., Jr.; Stratmann, R. E.; Burant, J. C.; Dapprich, S.; Millam, J. M.; Daniels, A. D.; Kudin, K. N.; Strain, M. C.; Farkas, O.; Tomasi, J.; Barone, V.; Cossi, M.; Cammi, R.; Mennucci, B.; Pomelli, C.; Adamo, C.; Clifford, S.; Ochterski, J.; Petersson, G. A.; Ayala, P. Y.; Cui, Q.; Morokuma, K.; Malick, D. K.; Rabuck, A. D.; Raghavachari, K.; Foresman, J. B.; Cioslowski, J.; Ortiz, J. V.; Baboul, A. G.; Stefanov, B. B.; Liu, G.; Liashenko, A.; Piskorz, P.; Komaromi, I.; Gomperts, R.; Martin, R. L.; Fox, D. J.; Keith, T.; Al-Laham, M. A.; Peng, C. Y.; Nanayakkara, A.; Challacombe, M.; Gill, P. M. W.; Johnson, B.; Chen, W.; Wong, M. W.; Andres, J. L.; Gonzalez, C.; Head-Gordon, M.; Replogle, E. S. and Pople, J. A., Gaussian, Inc., Pittsburgh, PA, 1998.

(27) Patchkovskii, S.; Thiel, W. *J. Mol. Model* **2000**, *6*, 67–75.

TABLE 3. NICS Values for Compounds **1**, **2**, **11**, **14**, **23**, **24**, **25**, and **26**

| point | 1 | 2 | 11 | 14 | 23 | 24 | 25 | 26 |
|-----------------|----------|----------|-----------|-----------|-----------|-----------|-----------|-----------|
| 1 | −14.73 | −12.81 | −18.91 | | −0.24 | −19.15 | | −15.13 |
| 2 | −15.22 | −12.98 | −17.66 | | −0.09 | −18.15 | | −15.45 |
| 3 | −13.52 | −11.75 | −17.66 | | −0.09 | −18.15 | | −13.78 |
| 4 | −14.73 | −12.81 | −18.91 | | −0.24 | −19.15 | | −15.13 |
| av ^a | −14.55 | −12.59 | −18.29 | | −0.07 | −18.65 | | −14.87 |
| 30 | −34.60 | −34.00 | −36.18 | | −27.02 | −36.28 | | −34.84 |
| 40 | −35.12 | −34.42 | −36.75 | | −27.12 | −36.84 | | −35.34 |
| 5 | 0.71 | −3.87 | | −8.12 | | | 0.88 | 0.67 |

^a Average value of points 1–4.

TABLE 4. Relative Aromaticities (%) of the DDP Nucleus of **1**, **2**, **11**, and **26**

| | RA _{exptl} | RA _{calcd} | RA _{NICS} ^a | RA _{NICS 30} ^b | RA _{NICS 40} ^c |
|-----------|---------------------|---------------------|---------------------------------|------------------------------------|------------------------------------|
| 1 | 89.7 | 78.6 | 78.1 | 81.9 | 82.3 |
| 2 | 93.5 | 70.1 | 67.6 | 75.4 | 75.1 |
| 11 | 98.1 | 96.0 | 98.1 | 98.9 | 99.1 |
| 26 | | 80.2 | 79.8 | 84.4 | 84.6 |

^a Relative aromaticity (%) calculated using NICS_{Av} minus the average of NICS points 1–4. ^b Relative aromaticity (%) calculated using NICS point 30. ^c Relative aromaticity (%) calculated using NICS point 40.

ODA (**n**) referenced to the *fully* aromatic parent (**14**) by means of eqs 4–6. We optimized the structures (Supporting Information Tables S1 and S2) of **1**, **2**, **14**, **25**, and **26** and used these geometries to calculate their NMR chemical shifts (¹H, Supporting Information Table S3; ¹³C, Supporting Information Table S4) and NICS values (Table 3) at the points shown (Figures 1 and 2). The RAs (Tables 4 and 5) were calculated from these data using eqs 1–6.

DDP nucleus:

$$RA_{\text{exptl}} = \frac{\delta(\mathbf{23}) - \delta(\mathbf{n})}{\delta(\mathbf{23}) - \delta(\mathbf{24})} \times 100 \quad (1)$$

$$RA_{\text{calcd}} = \frac{\delta_{\text{calcd}}(\mathbf{23}) - \delta_{\text{calcd}}(\mathbf{n})}{\delta_{\text{calcd}}(\mathbf{23}) - \delta_{\text{calcd}}(\mathbf{24})} \times 100 \quad (2)$$

$$RA_{\text{NICS}} = \frac{\text{NICS}(\mathbf{23}) - \text{NICS}(\mathbf{n})}{\text{NICS}(\mathbf{23}) - \text{NICS}(\mathbf{24})} \times 100 \quad (3)$$

RA_{exptl} = experimental relative aromaticity of DDP **n** (compared to **24**),

δ(**23**) = experimental ¹H chemical shift of the Me groups on **23** (0.97 ppm),

δ(**n**) = experimental ¹H chemical shift of the Me groups (average if different) on annelated DDP,

δ(**24**) = experimental ¹H chemical shift of the Me groups on **24** (−4.25 ppm),

RA_{calcd} = calculated relative aromaticity of DDP **n** (compared to **24**),

δ_{calcd}(**23**) = calculated ¹H chemical shift of the Me groups on **23** (1.09 ppm),

δ_{calcd}(**n**) = calculated ¹H chemical shift of the Me groups (average if different) on annelated DDP,

(28) Williams, R. V.; Armantrout, J. R.; Twamley, B.; Mitchell, R. H.; Ward, T. R.; Bandyopadhyay, S. *J. Am. Chem. Soc.* **2002**, *124*, 13495–13505.

(29) Forsyth, D. A.; Sebag, A. B. *J. Am. Chem. Soc.* **1997**, *119*, 9483–9494.

(30) Elbaum, D.; Nguyen, T. B.; Jorgensen, W. L.; Schreiber, S. L. *Tetrahedron* **1994**, *50*, 1503–1518.

TABLE 5. Relative Aromaticity (%) of the ODA Nucleus of **1**, **2**, and **26**

| | RA _{exptl} (H21) | RA _{calcd} (H21) | RA _{exptl} (H22) | RA _{calcd} (H22) | RA _{NICS 5} ^a |
|-----------|---------------------------|---------------------------|---------------------------|---------------------------|-----------------------------------|
| 1 | | | | | 1.9 |
| 2 | 85.1 | 98.1 | 51.3 | 68.0 | 52.78 |
| 26 | | | | | 2.33 |

^a Relative aromaticity (%) calculated using NICS point 5.

δ_{calcd}(**24**) = calculated ¹H chemical shift of the Me groups on **24** (−6.30 ppm),

RA_{NICS} = NICS relative aromaticity of DDP **n** (compared to **24**),

NICS(**23**) = NICS_{Av} or NICS value at point 30 or 40 for **23** (0.07, −27.02, and −27.12, respectively),

NICS(**n**) = NICS_{Av} or NICS value at point 30 or 40 for **n**, and

NICS(**24**) = NICS_{Av} or NICS value at point 30 or 40 for **24** (−18.65, −36.28, and −36.84, respectively).

ODA nucleus:

$$RA_{\text{exptl}} = \frac{\delta(\mathbf{25}) - \delta(\mathbf{n})}{\delta(\mathbf{25}) - \delta(\mathbf{14})} \times 100 \quad (4)$$

$$RA_{\text{calcd}} = \frac{\delta_{\text{calcd}}(\mathbf{25}) - \delta_{\text{calcd}}(\mathbf{n})}{\delta_{\text{calcd}}(\mathbf{25}) - \delta_{\text{calcd}}(\mathbf{14})} \times 100 \quad (5)$$

$$RA_{\text{NICS}} = \frac{\text{NICS}(\mathbf{25}) - \text{NICS}(\mathbf{n})}{\text{NICS}(\mathbf{25}) - \text{NICS}(\mathbf{14})} \times 100 \quad (6)$$

RA_{exptl} = experimental relative aromaticity of ODA **n** (compared to **14**),

δ(**25**) = experimental ¹H chemical shift of H21 or H22 on **25** (6.0 and 5.6 ppm, respectively),

δ(**n**) = experimental ¹H chemical shift of H21 or H22 on ODA **n**,

δ(**14**) = experimental ¹H chemical shift of H21 or H22 on **14** (7.92 and 7.39 ppm, respectively),

RA_{calcd} = calculated relative aromaticity of ODA **n** (compared to **14**),

δ_{calcd}(**25**) = calculated ¹H chemical shift of H21 or H22 on **25** (6.17 and 5.79 ppm, respectively),

δ_{calcd}(**n**) = calculated ¹H chemical shift of H21 or H22 on ODA **n**,

δ_{calcd}(**14**) = calculated ¹H chemical shift of H21 or H22 on **14** (8.32 and 7.79 ppm, respectively),

RA_{NICS} = NICS relative aromaticity of ODA **n** (compared to **14**),

NICS(**25**) = NICS value at point 5 for **25** (0.88),

NICS(**n**) = NICS value at point 5 for **n**, and

NICS(**14**) = NICS value at point 5 for **14** (−8.12).

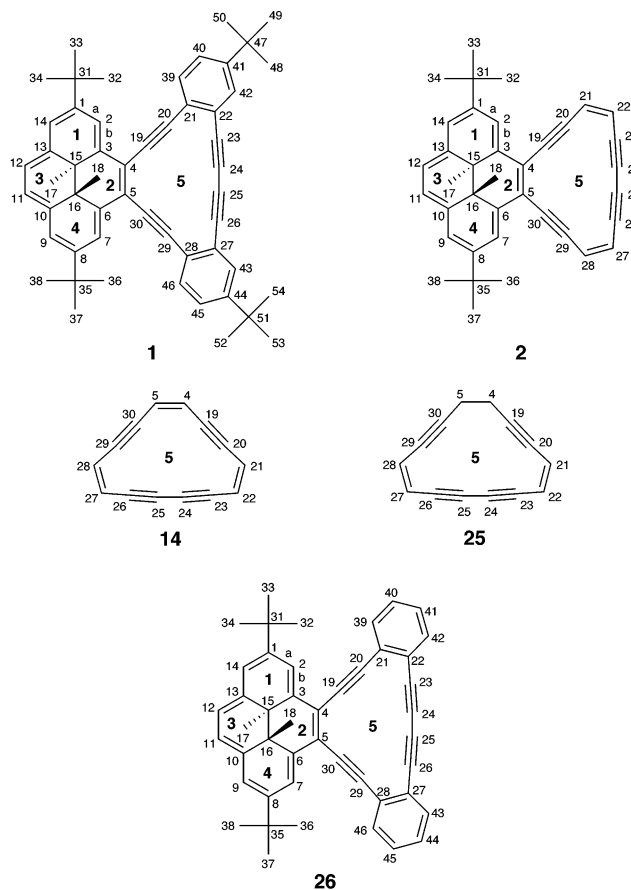


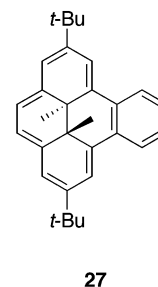
FIGURE 2. Numbering scheme and location of the NICS points for **1**, **2**, **14**, **25**, and **26**. NICS points are shown in bold type.

Comparison of the NICS (at point 5, Table 3) for the parent ODA (**14**) and the dihydro derivative **25**, in which cyclic delocalization is interrupted, clearly demonstrates that **14** should indeed be considered as aromatic. Similarly, this comparison also reveals that local anisotropies associated with the acetylenic bonds are minimal at point 5. We would thus expect fusion of an ODA to a DDP to result in a reduction in diatropicity of both systems, with the more diatropic DDP dominating the ODA, causing a greater attenuation in diatropicity of the ODA than the DDP. NICS_{Av} and NICS (point 5) for the hybrid **2** immediately confirm this hypothesis, with NICS_{Av} decreasing in magnitude from -18.29 in the di-*t*-Bu-DDP **11** to -12.59 in **2** and NICS (point 5) correspondingly decreasing from -8.12 to -3.87 in **14** and **2**, respectively. Again, as would be expected, fusion of two benzene rings to the ODA nucleus in **1** and **26** essentially kills the aromaticity of the ODA (NICS point 5, 0.71 and 0.67 , respectively) and restores much of the aromaticity of the DDP nucleus (NICS_{Av}, -14.55 and -14.87 , respectively). We previously found that RAs furnish a reliable ordering of aromaticity, but that their absolute magnitude is not of particular significance.²⁸ Examination of the RA_{exptl} values in Tables 4 and 5 shows that the (*experimental*) diatropicity of the di-*t*-Bu-DDP and ODA nuclei are decreased upon fusion to form the corresponding hybrid. Similarly, all calculated RAs support this conclusion and, in general, in agreement with our earlier findings,²⁸

suggest a greater reduction in diatropicity upon annelation for both nuclei than do the experimental RAs.

All three ODA–DDP hybrids exhibit essentially planar ODA and DDP nuclei, with their fusion resulting in a mutual tilting of these planes to give propeller-shaped molecules of C_2 symmetry. The calculated bond lengths reported in Tables S1 and S2 again indicate reduction in the diatropicity of both nuclei upon fusion of a DDP and an ODA. We introduced the alternance parameter ($\Delta\Sigma$ = average bond length of “a”-type bonds – average bond length of “b”-type bonds; see Figure 2 for identification of a- and b-type bonds) as a measure of the bond localization/reduction in the diatropicity of the DDP nucleus upon annelation.²⁸ The greater the magnitude of $\Delta\Sigma$, the more localized the DDP and hence the less diatropic. $\Delta\Sigma$ for **1**, **2**, and **26** (0.020 , 0.031 , and 0.019 , respectively) shows a degree of bond localization in the DDP nucleus of each of these hybrids entirely consistent with the reduced diatropicities indicated by experiment, NICS, and RAs. It is interesting to note that the variations in bond lengths in the ODA nuclei also show some localization upon annelation. The “single” bonds (4–19, 20–21, 22–23, 24–25, 26–27, 28–29, and 30–5) in **1**, **2**, and **26** each show a lengthening compared with those in **14**, while the “double” (21–22 and 27–28 in **2**) and “triple” (19–20, 23–24, 25–26, and 29–30) bonds exhibit a similar shortening in **1**, **2**, and **26** compared with those in **14**. This adjustment in bond lengths, as expected, is more apparent in **1** and **26** than in **2**.

It is illuminating to compare the results from the above applications of the various measures of aromaticity to those for the ODA–DDP hybrids and those previously reported for di-*t*-Bu-benzo[*e*]DDP (**27**).²⁸ The RAs of **27**



range from 48.9% (RA_{exptl}) to 25.2% (RA_{NICS(Av)}), and the alternance parameter, $\Delta\Sigma$, is -0.056 . Obviously, benzene is appreciably more aromatic than ODA **14** and, upon annelation to the di-*t*-Bu-DDP, is much more effective in bond localizing and reducing the diatropicity of the DDP nucleus.

Perusal of the ¹H and ¹³C chemical shifts presented in Tables S3 and S4 confirms that the B3LYP/6-31G* method provides good modeling of the DDPs/ODAs. The calculated shieldings are for a single conformer of each compound; we consequently averaged the predicted chemical shifts (obtained using eqs 7 and 8²⁹) for the symmetry-

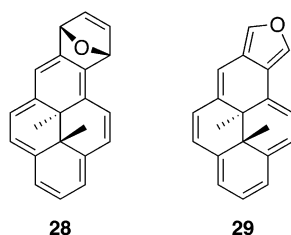
$$\delta_{\text{calcd}} = \sigma_{\text{TMS}} - \sigma \quad (7)$$

$$\delta_{\text{calcd}}(^{13}\text{C}) = -1.084\sigma + 203.1 \quad (8)$$

related ¹H and ¹³C atoms made equivalent by rotation of the Me and/or *t*-Bu groups. The agreement between

experimental and calculated ^1H chemical shifts is excellent. Experimental ^{13}C chemical shifts are only available for **1**, **14**, and **25**, where agreement between experiment and theory is very good. However, the calculated ^{13}C shifts for the acetylenic carbons in **14** show a significant deviation from experiment (by as much as 8.33 ppm). The assignments of experimental chemical shifts are, in the main, based on the best fit with the calculated data.

A consistent picture emerges from both theory and experiment. The ODA nucleus is weakly aromatic and causes bond localization with concomitant reduction in the diatropicity of the fused DDP; however, one puzzling aspect of this study persists. Experimentally the ^1H NMR chemical shift of the internal methyl groups of **1** is at lower field than that of **2**, suggesting that the degree of bond localization/reduction in the diatropicity of the DDP nucleus is greater in **1** than in **2**. Such a suggestion is clearly contrary to expectations and our calculated results in which all indicators of aromaticity (including the calculated ^1H chemical shifts for the internal methyls) firmly place the DDP nucleus of **1** as more aromatic than that of **2**. In most cases where the dihydropyrene nucleus has been used to probe aromaticity, the change in ring current caused by the fused system has been fairly large, and hence, the change in chemical shift observed for the methyl protons is also large, about 0.5 ppm for each 10% change in the ring current of the parent **24**.⁷ Generally, the anisotropy effects of substituents have been small,³¹ <0.3 ppm, and thus have been ignored. However, as the aromaticity of the fused system becomes small, this becomes more risky, and probably has little meaning at ring currents <10% of that of the parent, because then anisotropy effects may be playing a role. In our paper on bond fixation effects caused by fused oxabicyclic rings on the dihydropyrene system,³² several examples are given where the anisotropy effects are small, <0.3 ppm, such that the 0.8 ppm shift observed for **28** was deemed significant. Likewise the 0.8 ppm shift of the internal methyl protons of **29** from an acyclic model were deemed



significant.³³ In the current paper, the difference in the ^1H NMR chemical shifts of the internal methyl protons of **1** (δ -3.71) and **2** (δ -3.91) is only 0.2 ppm, and also the differences between **1** and **2** and their respective acyclic precursors **10** (0.06 ppm) and **13** (0.23 ppm) all fall below the 0.3 ppm advisory limit, and so should not be used to resolve such finely balanced differences in aromaticity that are found here.

(31) Mitchell, R. H. In *Advances in Theoretically Interesting Molecules*; Thummel, R. P., Ed.; JAI Press Inc.: Stamford, CT, 1989; Vol. 1, pp 135–199.

(32) Mitchell, R. H.; Chen, Y.; Iyer, V. S.; Lau, D. Y. K.; Baldrige, K. K.; Siegel, J. S. *J. Am. Chem. Soc.* **1996**, *118*, 2907–2911.

(33) Mitchell, R. H.; Zhou, P. *Tetrahedron Lett.* **1991**, *44*, 6319–6322.

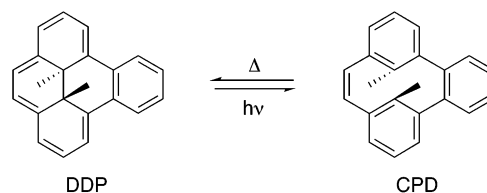


FIGURE 3. Switching between the DDP and CPD forms.

Photochemical Properties. The fused annulenes prepared above did not modify the ring currents in the DDP rings significantly, at least as estimated by the internal methyl chemical shifts, despite the calculated aromaticity of the DBA parts. We wondered whether the photochemical properties of the DDP nucleus would thus be modified. The DDP nucleus behaves as a photochemical switch. The properties of this switch are dramatically changed by fusion of arenes along the faces of the DDP.^{13,34} Fusion of a single benzene ring as in **27** facilitates rapid isomerization between the closed (DDP) form and the open cyclophanediene (CPD) form (Figure 3). When benzene rings are fused on opposite faces, the cyclophane dominates and the pyrene can only be seen for a short time at low temperature. The pyrene core itself, however, is much more stable than its cyclophane analogue, and the cyclophane can only be achieved with difficulty. Fused DBA–DDP hybrids are thus of obvious interest, since the photochemical properties might be between the two extremes.

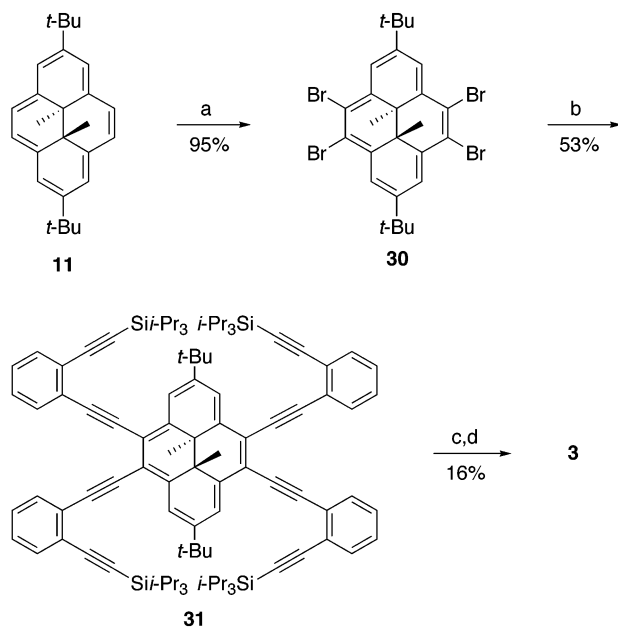
With the above in mind, bisfused DBA–DDP hybrids were synthesized to help fine-tune the isomerization of the pyrene to the cyclophane. Our initial efforts were directed toward hybrids **3** and **32**.¹⁶ Both systems were synthesized from a common starting compound, tetrabromide **30**,³⁵ obtained by tetrahalogenation of DDP **11** (Scheme 5). For hybrid **3**, excess 1-ethynyl-2-(triisopropylsilyl)ethynylbenzene^{8b} was reacted with **30** using Pd-mediated conditions to provide α,ω -polyynes **31**. Desilylation using Bu_4NF and cyclization with CuCl in pyridine gave **3** in 8% overall yield.

As with the attempted synthesis of **19**, hybrid **32** was assembled through sequential acetylene–haloarene and acetylene–acetylene cross-couplings. Reaction of **30** with excess (dimethylthexylsilyl)acetylene afforded tetrayne **33** in 33% yield (Scheme 6). After removal of the silyl protecting groups with Bu_4NF , the tetrayne was coupled to 4 equiv of 1-bromoethynyl-2-(triisopropylsilyl)ethynylbenzene^{8b} to give polyynes **34**. Desilylation and cyclization in a $\text{Cu}(\text{OAc})_2/\text{pyridine}$ mixture furnished **32** in 12% overall yield.

^1H NMR spectra revealed a downfield shift of the interior methyl protons in comparison with their precyclized, desilylated synthons. The aromaticity of the two fused [14]- and [18]annulenes, however, could not be directly related to this shift because of competitive resonance. For hybrids **3** and **32**, the two annulenes are fused in such a way that for one annulene to bond fix the DDP would result in the other annulene being bond

(34) (a) Mitchell, R. H.; Ward, T. R.; Wang, Y.; Dibble, P. W. *J. Am. Chem. Soc.* **1999**, *121*, 2601–2602. (b) Mitchell, R. H. *Eur. J. Org. Chem.* **1999**, 2695–2703.

(35) Tashiro, M.; Yamato, T. *J. Am. Chem. Soc.* **1982**, *104*, 3701–3707.

SCHEME 5^a

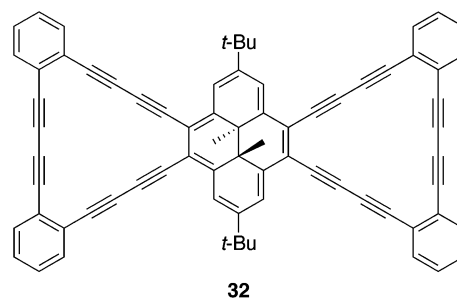
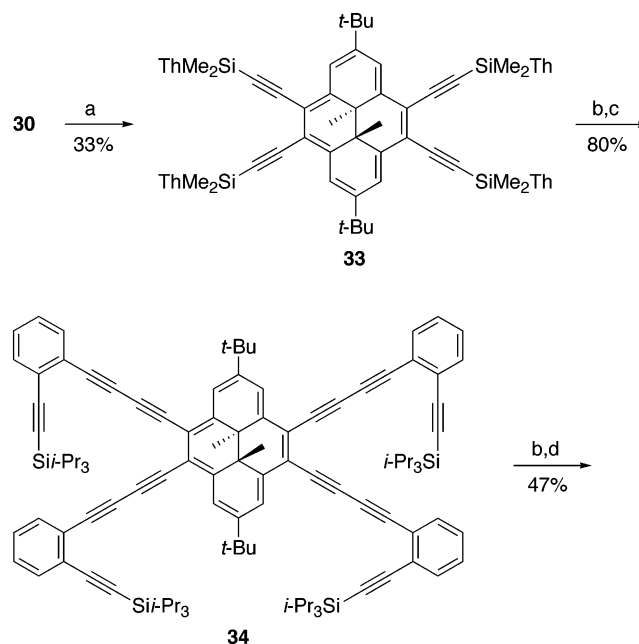
^a Reagents and conditions: (a) Br₂, CCl₄; (b) 1-ethynyl-2-(triisopropylsilyl)ethynylbenzene, PdCl₂(PPh₃)₂, Pd(PPh₃)₄, CuI, DMF, Et₃N, 100 °C; (c) Bu₄NF, THF, MeOH; (d) CuCl, THF, pyridine.

fixed as well. This can be confirmed by comparing the interior methyl shifts of our systems ($\delta(\text{Me})$ -3.33 ppm for **3** and -3.49 ppm for **32**) with that of the analogous bis(benzene-fused) DDP ($\delta(\text{Me})$ -3.41 ppm).^{13c} Further comparison of **3** with a similar structure, tetra(phenylethynyl)-DDP **35**, obtained from the coupling of desilylated **33** with excess iodobenzene (Scheme 7), shows virtually identical shifts for their interior methyl protons ($\delta(\text{Me})$ -3.32 ppm for **35**).

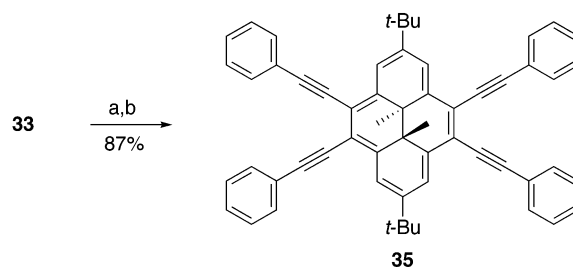
UV–vis analysis of the two bisfused hybrids revealed an absorption in the long-wavelength region (Figure 4). Since previous photoisomerization results using the DDP core showed isomerization using light at ~ 360 nm (for the CPD) and ~ 450 nm (for the DDP), this would allow for the system to be “read” at a third wavelength that should not cause unwanted scrambling of information. Photoisomerization studies, however, were unsuccessful in that the CPD could not be obtained efficiently because of extremely facile reversion to the pyrene form.

Substituting a benzene ring for one annulene should slow the ring-closing electrocyclization reaction. The resultant molecule, DBA–DDP hybrid **4**, was constructed analogously to **1**. NBS bromination of benzo-DDP **27**¹⁷ furnished light-sensitive dibromide **36** in 48% yield (Scheme 8). Sonogashira coupling of **36** with excess 1-ethynyl-2-(triisopropylsilyl)ethynylbenzene^{8b} in Et₃N and DMF provided polyene **37** in 77% yield. Desilylation and cyclization using CuCl in pyridine gave hybrid **4** as a dark purple solid in 33% overall yield.

As before, ¹H NMR analysis revealed an upfield shift of the internal methyl protons relative to those of the uncyclized polyene ($\delta(\text{Me})$ -1.24 for **37** and -1.32 for **4**). Photoisomerization, however, could be effected using light from an overhead projector (to induce cyclophane formation) and light from a UV lamp (to induce pyrene

SCHEME 6^a

^a Reagents and conditions: (a) Me₂ThSiC≡CH, PdCl₂(PPh₃)₂, Pd(PPh₃)₄, CuI, DMF, Et₃N, 100 °C; (b) Bu₄NF, THF, MeOH; (c) 1-(bromoethynyl)-2-(triisopropylsilyl)ethynylbenzene, Pd(dba)₂, CuI, LiI, DMSO, 1,2,2,6,6-pentamethylpiperidine; (d) Cu(OAc)₂, THF, pyridine. Th = thexyl = 1,1,2-trimethylpropyl.

SCHEME 7^a

^a Reagents and conditions: (a) Bu₄NF, THF, MeOH; (b) PhI, PdCl₂(PPh₃)₂, Pd(PPh₃)₄, CuI, Et₃N.

formation). Both isomers were stable under ambient conditions. Photoswitching could be achieved within a few minutes in an NMR tube. The UV–vis spectra of **4** and its CPD analogue **38** are shown in Figure 5, which depicts a significant decrease in the absorption at 450 nm and increase in the absorption at 320 nm in going from the DDP to the CPD form. Unfortunately, neither state absorbs appreciably in the 600–800 nm range, where these systems are intended to be read.

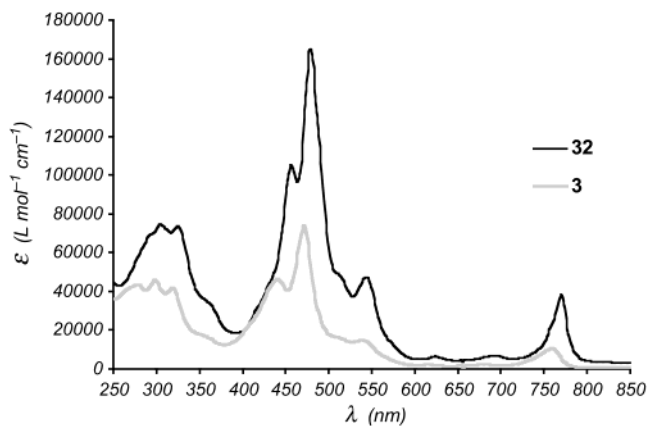
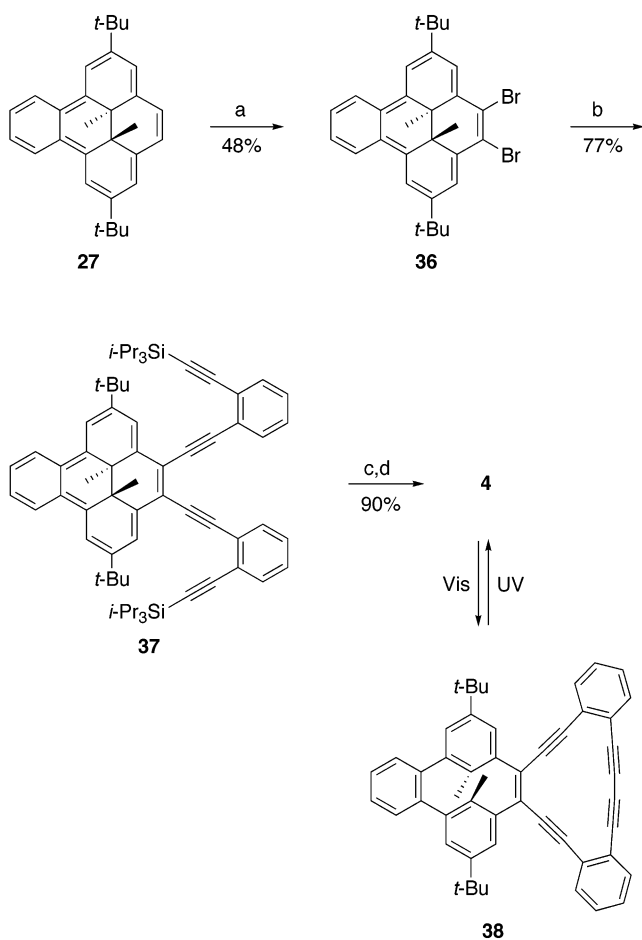


FIGURE 4. Electronic absorption spectra of hybrids **3** and **32**.

SCHEME 8^a



^a Reagents and conditions: (a) NBS, DMF, CH₂Cl₂; (b) 1-ethynyl-2-(triisopropylsilyl)ethynylbenzene, PdCl₂(PPh₃)₂, Pd(PPh₃)₄, CuI, DMF, Et₃N, 100 °C; (c) Bu₄NF, MeOH, THF; (d) CuCl, pyridine, MeOH, THF.

Conclusions

The synthesis of mono- and bisfused DBA–DDP hybrids has been accomplished. Comparison of the interior methyl resonances for the DDP core, its arene resonances, and its calculated RAs all confirm the existence of weak diatropic ring currents associated with the ODA nucleus. In agreement with expectations, the calculated

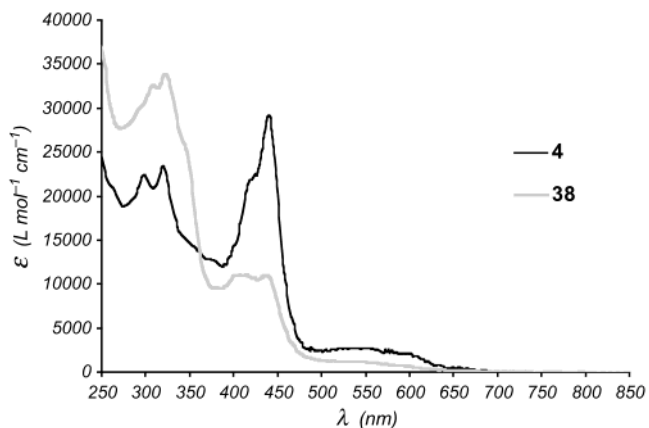


FIGURE 5. Electronic absorption spectra of DDP **4** and its corresponding CPD form **38**.

data, NICS and bond lengths, clearly demonstrate that the DDP-fused ODA nucleus in **2** is considerably more diatropic than the ODA nucleus in **1**, fused with a DDP and two benzenes. The experimental ¹H NMR chemical shifts of the internal methyls of the DDPs in **1** and **2** only differ by 0.2 ppm, which is on the same order as anisotropy-driven perturbations to these methyl shifts. We conclude that such shift differences of less than 0.3 ppm for the internal methyls of the DDP nucleus are too small to reliably measure the relative aromaticity of the DDP nucleus and, subsequently, the annelating group. Hybrids where both a benzene ring and a [14]DBA are fused to the DDP allow for facile isomerization between the pyrene and cyclophanediene isomers using different light sources.

Experimental Section

General Information. ¹H and ¹³C NMR spectra were recorded on a 300 MHz (¹H, 299.95 MHz; ¹³C, 75.43 MHz) or 360 MHz (¹H, 360 MHz; ¹³C, 90.6 MHz) NMR spectrometer and were obtained in CDCl₃. Chemical shifts (δ) are expressed in parts per million downfield from tetramethylsilane using the residual chloroform (¹H, 7.26 ppm; ¹³C, 77.0 ppm) as internal standard. Coupling constants are expressed in hertz. Et₃N was distilled from CaH₂ under a N₂ atmosphere prior to use. THF and Et₂O were distilled from Na and benzophenone under a N₂ atmosphere prior to use. All other chemicals were of reagent quality and used as obtained from the manufacturers. Column chromatography was performed on reagent grade silica gel (230–400 mesh). Precoated silica gel plates were used for analytical (200 × 50 × 0.25 mm) and preparative (200 × 200 × 1 mm) thin-layer chromatography. Reactions were carried out in an inert atmosphere (dry N₂ or Ar) when necessary. All deprotected terminal alkynes were used directly without further purification.

General Procedure A. Coupling Acetylenes to Bromo-DDPs. The bromo-DDP (1 equiv), PdCl₂(PPh₃)₂ (0.04 equiv), Pd(PPh₃)₄ (0.02 equiv), and CuI (0.14 equiv) were suspended in Et₃N and DMF (2:1 v/v, 0.15 M) in a glass pressure tube. The acetylene (1.2 equiv per bromine) was added, and the contents were degassed by three successive freeze–pump–thaw cycles. The tube was then charged with N₂ and sealed. The mixture was heated to 100 °C for 24–48 h with stirring. After cooling, the mixture was diluted into Et₂O and washed successively with saturated NH₄Cl solution, H₂O, and brine. The organics were dried (MgSO₄) and vacuum filtered through silica gel. The solvent was evaporated, and the crude product was purified by either column or preparative thin-layer chromatography to give the final product in pure form.

General Procedure B. Cleavage of Silyl Protecting Groups Using Bu₄NF. The silyl-protected arylacetylene was dissolved in THF and MeOH (5:1 v/v, 0.03 M). Bu₄NF (1.0 M in THF, 3 equiv per silyl group) was added and the solution stirred overnight. The contents were diluted with Et₂O, washed with saturated NH₄Cl solution and brine, dried (MgSO₄), and vacuum filtered through silica gel. After evaporation, the crude desilylated product was used for subsequent coupling.

2,7-Di-*tert*-butyl-4-trimethylsilyl-*trans*-10b,10c-dimethyl-10b,10c-dihydropyrene (7). BuLi (4.0 mL, 2.5 M in hexanes) was added dropwise by syringe to vacuum-dried bromopyrene **6**¹⁷ (626 mg, 1.5 mmol) in dry THF (120 mL) at -78 °C. The initially green solution rapidly turned brown. The mixture was stirred for 7 min, and then freshly distilled Me₃-SiCl (3.0 mL, 28 mmol) was added carefully by syringe. Cooling was then stopped, and the reaction mixture gradually turned green. After the mixture was stirred for 30 min at 20 °C, hexanes and water were added. The organic phase was washed successively with 10% aq NaHCO₃ solution and water, dried (MgSO₄), and evaporated to give a green solid containing a ca. 7:1 mixture of **7** and **6**. The crude material was purified by chromatography on silica gel (hexanes) deactivated with 5% water. The leading green band was collected, and each fraction evaporated separately and analyzed by NMR. The fractions with over 96 mol % **7** were combined to give 292 mg. The remaining fractions were evaporated and rechromatographed to yield an additional 186 mg. The total purified yield was 478 mg (78%). Recrystallization (cyclohexane) of **7** gave green crystals: mp 186–188 °C; ¹H NMR (CDCl₃) δ 8.75 (d, *J* = 1.0 Hz, 1H), 8.66 (s, 1H), 8.51 (s, 1H), 8.49 (br s, 1H), 8.48 (br s, 1H), 8.40 (ABm, *J* = 7.7 Hz, 1H), 8.38 (ABm, 1H), 1.68 (s, 9H), 1.67 (s, 9H), 0.67 (s, 9H), -4.02 (s, 3H), -4.05 (s, 3H); ¹³C NMR (CDCl₃) δ 145.26, 145.23, 141.01, 135.48, 136.22, 135.65, 133.08, 129.54, 122.54, 122.33, 121.55, 121.20, 120.74, 120.06, 36.09, 35.90, 31.95, 30.30, 29.24, 14.57, 14.33, 1.04; IR (KBr) ν 1382, 1358, 1342, 1249, 1227, 874, 849, 835, 669 cm⁻¹; MS (CI) *m/z* (rel intens) 417 (100, M⁺ + H). Anal. Calcd for C₂₉H₄₀-Si: C, 83.59; H 9.68. Found: C, 83.56; H, 9.65.

4,5-Dibromo-2,7-di-*tert*-butyl-9-trimethylsilyl-*trans*-10b,10c-dimethyl-10b,10c-dihydropyrene (8). NBS (334 mg, 1.9 mmol) in dry DMF (40 mL) was added dropwise at 0 °C to a solution of **7** (253 mg, 0.61 mmol) in dry CH₂Cl₂ (200 mL) under argon. After the addition, the ice bath was removed and the mixture allowed to stir for 20 h. The solution was diluted with hexanes, and then water was added with rapid stirring. After the solution was stirred for 2 min, the organic phase was washed with water, dried (MgSO₄), and concentrated. The residue was taken up in hexanes/CH₂Cl₂ (1:1) and filtered through silica gel deactivated with 5% water. Removal of the solvent furnished **8** (330 mg, 95%). Recrystallization from cyclohexane gave green crystals: mp 203–206 °C; ¹H NMR (CDCl₃) δ 8.90 (d, *J* = 1.1 Hz, 1H), 8.88 (d, *J* = 1.3 Hz, 1H), 8.75 (d, *J* = 0.9 Hz, 1H), 8.63 (s, 1H), 8.50 (br s, 1H), 1.69 (s, 9H), 1.68 (s, 9H), 0.66 (s, 9H), -3.76 (s, 3H), -3.78 (s, 3H); ¹³C NMR (CDCl₃) δ 148.43, 148.30, 142.11, 137.03, 135.04, 134.98, 132.83, 131.22, 123.02, 122.87, 122.84, 122.31, 118.91, 118.67, 36.47, 36.28, 33.20, 32.11, 31.80, 14.53, 14.34, 0.92; IR (KBr) ν 1362, 1337, 1248, 965, 873, 848, 837, 749, 662 cm⁻¹; MS (CI) *m/z* 573 (M⁺ + H, correct isotope pattern). Anal. Calcd for C₂₉H₃₈Br₂Si: C, 61.63; H 6.67. Found: C, 61.72; H, 6.74.

4,5-Dibromo-2,7-di-*tert*-butyl-*trans*-10b,10c-dimethyl-10b,10c-dihydropyrene (5). A solution of **8** (93 mg, 0.16 mmol) in THF (20 mL) was refluxed with Bu₄NF (1.5 mL, 1.0 M in THF) under argon for 24 h. After cooling, the mixture was diluted with hexanes and washed with water. The organic phase was dried (MgSO₄) and concentrated. The residue was taken up in hexane and CH₂Cl₂ (6:1 v/v) and filtered through silica gel deactivated with 5% water. The first band was collected and recrystallized (cyclohexane) to yield **5** (68 mg, 84%) as green crystals: mp 198–200 °C; ¹H NMR (CDCl₃) δ 8.96 (d, *J* = 1.3 Hz, 2H), 8.54 (d, *J* = 1.3 Hz, 2H), 8.45 (s, 2H),

1.69 (s, 18H), -3.82 (s, 6H); ¹³C NMR (CDCl₃) δ 148.32, 137.85, 133.20, 124.10, 123.21, 122.30, 119.15, 36.30, 32.15, 31.87, 14.24; IR (KBr) ν 1362, 1339, 874, 673 cm⁻¹; MS (CI) *m/z* 501 (M⁺ + H, correct isotope pattern). Anal. Calcd for C₂₆H₃₀Br₂: C, 62.17; H 6.02. Found: C, 62.84; H, 5.97. (About 3% bromopyrene **8** was present by ¹H NMR.)

4-*tert*-Butyl-1-ethynyl-2-(triisopropylsilyl)ethynylbenzene (9). A mixture of 4-*tert*-butyl-1-iodo-2-(triisopropylsilyl)ethynylbenzene¹⁸ (881 mg, 2.0 mmol), PdCl₂(PPh₃)₂ (42 mg, 0.06 mmol), CuI (19 mg, 0.10 mmol), and Et₃N (10 mL) was degassed by three freeze-pump-thaw cycles. Ethynyltrimethylsilane (0.56 mL, 4.0 mmol) was added and the mixture stirred at 40 °C for 10 h. The reaction was diluted with hexanes and filtered through a pad of Celite and silica gel. The filtrate was concentrated and the residue redissolved in THF (25 mL) and MeOH (5 mL). K₂CO₃ (276 mg, 2.0 mmol) was added and the mixture stirred at rt for 4 h. The reaction was diluted with hexanes and washed repeatedly with water and brine. The organic layer was dried (MgSO₄), filtered, and concentrated. Purification by column chromatography (hexanes) gave **9** (568 mg, 84%) as a yellow oil: ¹H NMR (CDCl₃) δ 7.47 (d, *J* = 2.1 Hz, 1H), 7.42 (d, *J* = 8.1 Hz, 1H), 7.29 (dd, *J* = 8.1, 2.1 Hz, 1H), 3.20 (s, 1H), 1.30 (s, 9H), 1.15 (s, 21H); ¹³C NMR (CDCl₃) δ 151.68, 132.21, 129.18, 126.21, 125.37, 122.17, 105.38, 94.35, 82.40, 80.29, 34.69, 30.99, 18.71, 11.31; IR (neat) ν 3304, 3062, 2159, 1463 cm⁻¹; HRMS *m/z* calcd for C₂₃H₃₄Si, 338.2430, found 338.2423.

Mono[14]DBA-*DDP* Polyene 10. Dibromide **5** (45 mg, 0.09 mmol), diyne **9** (140 mg, 0.41 mmol), PdCl₂(PPh₃)₂ (5.2 mg, 0.007 mmol), Pd(PPh₃)₄ (4.3 mg, 0.004 mmol), CuI (3 mg, 0.02 mmol), Et₃N (1 mL), and DMF (2 mL) were reacted using general procedure A. Column chromatography (petroleum ether) gave **10** (80 mg, 88%) as a tan oil: ¹H NMR (CDCl₃) δ 9.05 (s, 2H), 8.46 (s, 2H), 8.39 (s, 2H), 7.63 (d, *J* = 8.1 Hz, 2H), 7.55 (d, *J* = 1.8 Hz, 2H), 7.29 (dd, *J* = 8.1, 1.8 Hz, 2H), 1.66 (s, 18H), 1.34 (s, 18H), 0.94 (s, 21H), 0.93 (s, 21H), -3.65 (s, 6H); ¹³C NMR (CDCl₃) δ 150.46, 147.53, 138.33, 137.12, 132.68, 129.41, 125.34, 125.06, 124.42, 123.84, 122.08, 120.43, 117.17, 106.54, 96.59, 93.87, 91.78, 36.14, 34.64, 31.80, 31.10, 18.66, 11.25; IR (neat) ν 3035, 2958, 2197, 2153 cm⁻¹; UV-vis (CH₂Cl₂) λ_{max} (log ε) 380 (4.65), 414 (4.67), 484 (3.90), 683 (3.42) nm; HRMS *m/z* calcd for C₇₂H₉₆Si₂ 1016.7051, found 1016.7032.

Mono[14]DBA-*DDP* 1. Polyene **10** (66 mg, 0.065 mmol) was treated with Bu₄NF (1.5 mL, 1.5 mmol) in THF (15 mL) and MeOH (1 mL) using general procedure B. The desilylated polyene was dissolved in THF (8 mL) and added over 8 h to a slurry of CuCl (400 mg, 4.04 mmol), MeOH (2 mL), and pyridine (10 mL) under air at rt. After the solution was stirred for 48 h, the volatiles were evaporated and the crude material was redissolved in CH₂Cl₂ and vacuum filtered through silica gel. Purification by column chromatography (6:1 petroleum ether/CH₂Cl₂) gave **1** (14 mg, 30%) as a dark red powder: mp > 350 °C; ¹H NMR (CDCl₃) δ 9.54 (s, 2H), 8.59 (s, 2H), 8.48 (s, 2H), 8.22 (d, *J* = 8.1 Hz, 2H), 7.65 (d, *J* = 1.5 Hz, 2H), 7.61 (dd, *J* = 8.1, 1.5 Hz, 2H), 1.82 (s, 18H), 1.41 (s, 18H), -3.71 (s, 6H); ¹³C NMR (CDCl₃) δ 150.90, 147.95, 139.13, 138.75, 132.50, 128.08, 126.27, 126.14, 124.07, 122.31, 121.95, 121.48, 115.04, 99.61, 93.81, 87.14, 80.09, 36.53, 34.94, 32.12, 31.14, 15.02; IR (KBr) ν 3046, 2961, 2924, 2865, 2207, 2160 cm⁻¹; UV-vis (CH₂Cl₂) λ_{max} (log ε) 313 (4.86), 359 (4.49), 407 (4.89), 437 (4.98), 506 (4.13), 577 (2.93), 636 (3.10), 704 (3.96) nm; HRMS *m/z* calcd for C₅₄H₅₄ 702.4226, found 702.4237.

Mono[14]alkene-*DDP* Polyene 13. Dibromo-*DDP* **5** (40 mg, 0.08 mmol), enediyne **12**²⁰ (79 mg, 0.34 mmol), PdCl₂(PPh₃)₂ (3.4 mg, 0.0048 mmol), Pd(PPh₃)₄ (2.8 mg, 0.0024 mmol), CuI (1.7 mg, 0.0088 mmol), Et₃N (1 mL), and DMF (2 mL) were reacted using general procedure A. Purification by column chromatography (19:1 petroleum ether/CH₂Cl₂) gave **13** (15 mg, 23%) as a viscous, dark red oil: ¹H NMR (CDCl₃) δ 8.95 (s, 2H), 8.46 (s, 2H), 8.39 (s, 2H), 6.41 (d, *J* = 11.1 Hz, 2H), 6.00 (d, *J* = 11.1 Hz, 2H), 1.68 (s, 18H), 1.25 (s, 42H),

–3.71 (s, 6H); ^{13}C NMR (CDCl_3) δ 147.93, 138.51, 137.24, 124.16, 122.31, 121.27, 120.30, 118.39, 116.09, 104.54, 99.36, 96.69, 95.31, 36.16, 31.74, 18.59, 15.09, 11.17; IR (neat) ν 3037, 2956, 2864, 2181, 2139 cm^{-1} ; UV–vis (CH_2Cl_2) λ_{max} (log ϵ) 262 (4.32), 313 (4.08), 384 (4.45), 413 (4.48), 490 (3.73), 687 (3.12) nm; HRMS m/z calcd for $\text{C}_{56}\text{H}_{76}\text{Si}_2$ 804.5486, found 804.5479.

Mono[14]alkene–DDP 2. Polyynes **13** (15 mg, 0.019 mmol) was treated with Bu_4NF (1.5 mL, 1.5 mmol) in MeOH (0.7 mL) and THF (6 mL) using general procedure B. The desilylated product was dissolved in THF (3 mL) and added over 8 h to a slurry of CuCl (38 mg, 0.37 mmol), MeOH (1 mL), and pyridine (8 mL) under air at rt. After the solution was stirred for an additional 48 h, the volatiles were evaporated and the contents were redissolved in CH_2Cl_2 and vacuum filtered through silica gel. Purification by preparative TLC (9:1 petroleum ether/ CH_2Cl_2) gave **2** (3.5 mg, 38%) as an unstable red oil: ^1H NMR (CDCl_3) δ 9.65 (s, 2H), 8.69 (s, 2H), 8.58 (s, 2H), 7.66 (d, J = 9.0 Hz, 2H), 6.61 (d, J = 9.0 Hz, 2H), 1.80 (s, 18H), –3.91 (s, 6H); IR (neat) ν 3038, 2156, 2109 cm^{-1} ; UV–vis (CH_2Cl_2) λ_{max} (log ϵ) 312 (4.49), 400 (4.49), 443 (4.44), 718 (3.74) nm; MS (FAB) m/z (rel intens) 491.2 (50, M^+ + H^+), 282.3 (100, M^+ + Na – $\text{C}_{18}\text{H}_{15}$).

Mono[14]alkane–DDP Polyynes 18. Dibromo **5** (20 mg, 0.04 mmol), diyne **17**²¹ (180 mg, 1.2 mmol), $\text{PdCl}_2(\text{PPh}_3)_2$ (3.4 mg, 0.0048 mmol), $\text{Pd}(\text{PPh}_3)_4$ (2.8 mg, 0.0024 mmol), CuI (1.7 mg, 0.0088 mmol), Et_3N (1 mL), and DMF (2 mL) were reacted using general procedure A. Purification by column chromatography (9:1 petroleum ether/ CH_2Cl_2) gave **18** (23 mg, 92%) as a dark yellow oil: ^1H NMR (CDCl_3) δ 8.94 (s, 2H), 8.46 (s, 2H), 8.38 (s, 2H), 3.06–3.00 (m, 4H), 2.85–2.80 (m, 4H), 1.68 (s, 18H), 0.17 (s, 18H), –3.80 (s, 6H); ^{13}C NMR (CDCl_3) δ 147.47, 138.21, 136.92, 123.79, 121.87, 120.13, 116.70, 105.67, 96.60, 85.68, 80.71, 36.17, 31.84, 20.88, 20.70, 14.92, 0.10; IR (neat) ν 3036, 2959, 2923, 2864, 2176 cm^{-1} ; UV–vis (CH_2Cl_2) λ_{max} (log ϵ) 273 (3.87), 365 (4.56), 405 (4.49), 479 (3.52), 500 (3.52), 681 (2.82) nm; HRMS m/z calcd for $\text{C}_{44}\text{H}_{56}\text{Si}_2$ 640.3921, found 640.3928.

Mono[14]alkane–DDP 16. Polyynes **18** (23 mg, 0.036 mmol) was combined with K_2CO_3 (276 mg, 2 mmol), MeOH (2 mL), and THF (7 mL) and stirred overnight at rt. The mixture was diluted with Et_2O and washed with H_2O . The organic layer was dried (MgSO_4), vacuum filtered through silica gel, and concentrated. The crude product was then dissolved in THF (3 mL) and added over 8 h to a slurry of CuCl (50 mg, 0.51 mmol), MeOH (2 mL), and pyridine (6 mL) under air at rt. After the solution was stirred for an additional 48 h, the volatiles were evaporated and the crude solid was redissolved in CH_2Cl_2 and vacuum filtered through silica gel. Purification by preparative TLC (3:1 petroleum ether/ CH_2Cl_2) provided **16** (3 mg, 17%) as a yellow semisolid: ^1H NMR (CDCl_3) δ 9.06 (s, 2H), 8.46 (s, 2H), 8.38 (s, 2H), 3.22 (t, J = 6.6 Hz, 4H), 2.68 (t, J = 6.6 Hz, 4H), 1.69 (s, 18H), –3.77 (s, 6H); ^{13}C NMR (CDCl_3) δ 147.44, 138.64, 138.09, 123.71, 121.85, 120.74, 120.66, 116.41, 96.75, 83.50, 81.17, 70.44, 36.15, 31.85, 29.69, 19.78, 14.90; IR (neat) ν 3040, 2955, 2924, 2853, 2257 cm^{-1} ; UV–vis (CH_2Cl_2) λ_{max} (log ϵ) 369 (4.73), 405 (4.65), 481 (3.81), 500 (3.81), 682 (3.40) nm; HRMS m/z calcd for $\text{C}_{38}\text{H}_{38}$ 494.2974, found 494.2970.

4,5-Bis(trimethylsilylethynyl)-2,7-di-tert-butyl-trans-10b,10c-dimethyl-10b,10c-dihdropyrene (20). Dibromo-**DDP 5** (50 mg, 0.1 mmol), ethynyltrimethylsilane (0.25 mL, 1.8 mmol), $\text{PdCl}_2(\text{PPh}_3)_2$ (4 mg, 0.0057 mmol), $\text{Pd}(\text{PPh}_3)_4$ (2.3 mg, 0.0020 mmol), CuI (3 mg, 0.016 mmol), Et_3N (1 mL), and DMF (2 mL) were reacted using general procedure A. Purification by column chromatography (9:1 hexanes/ CH_2Cl_2) gave **20** (33 mg, 61%) as a brown semisolid: ^1H NMR (CDCl_3) δ 9.02 (d, J = 1.4 Hz, 2H), 8.47 (d, J = 1.4 Hz, 2H), 8.39 (s, 2H), 1.69 (s, 18H), 0.45 (s, 18H), –3.76 (s, 6H); ^{13}C NMR (CDCl_3) δ 148.12, 138.69, 137.85, 124.19, 122.19, 120.53, 115.98, 104.01, 102.85, 36.25, 31.75, 15.05, 0.43; IR (neat) ν 3034, 2961, 2925, 2901, 2864, 2143 cm^{-1} ; UV–vis (CH_2Cl_2) λ_{max} (log ϵ) 278 (4.04),

370 (4.76), 407 (4.70), 483 (3.90), 684 (3.47) nm; HRMS m/z calcd for $\text{C}_{36}\text{H}_{48}\text{Si}_2$ 536.3295, found 536.3293.

Bis(DDP)–Dehydro[12]annulene 21 and Tris(DDP)–Dehydro[18]annulene 22. Diyne **20** (38 mg, 0.07 mmol) was dissolved in THF (2 mL) and MeOH (0.1 mL) and then treated with Bu_4NF (0.5 mL, 1.0 M in THF) using general procedure B. After workup, the crude desilylated diyne was dissolved in THF (2 mL) and DMSO (2 mL) and added to an argon-degassed mixture of 1-bromoethynyl-2-(triisopropylsilyl)ethynylbenzene^{8b} (72 mg, 0.2 mmol), $\text{Pd}(\text{dba})_2$ (3.5 mg, 0.006 mmol), CuI (1.0 mg, 0.005 mmol), LiI (7.5 mg, 0.04 mmol), and DMSO (2 mL) using the procedure of Vasella.²⁴ The reactants were stirred for 5 min at rt, and then 1,2,2,6,6-pentamethylpiperidine (87 mg, 0.56 mmol) was added. After 48 h, Et_2O (35 mL) and 10% aq NH_4Cl solution (10 mL) were added. The organic layer was washed with water, dried (MgSO_4), filtered, and concentrated. Purification by preparative TLC (4:1 petroleum ether/ CH_2Cl_2) gave **21** (5 mg, 19%) as an unstable red semisolid and **22** (12 mg, 44%) as a red solid. Data for **21**: ^1H NMR (CDCl_3) δ 8.66 (br s, 4H), 8.33 (br s, 4H), 8.27 (d, J = 2.1 Hz, 4H), 1.70 (s, 36H), –3.24 (s, 6H), –3.25 (s, 6H); IR (neat) ν 3036, 2963, 2157, 1467, 1261 cm^{-1} ; UV–vis (CH_2Cl_2) λ_{max} (log ϵ) 381 (5.02), 435 (4.79), 482 (4.96), 536 (4.56), 703 (3.80), 744 (4.15) nm; HRMS m/z calcd for $\text{C}_{60}\text{H}_{60}$ + H 781.4773, found 781.4795. Data for **22**: ^1H NMR (CDCl_3) δ 9.29 (s, 6H), 8.57 (s, 6H), 8.48 (s, 6H), 1.84 (s, 54H), –3.56 (s, 9H), –3.57 (s, 9H); IR (neat) ν 3036, 2924, 2177, 1464, 1070 cm^{-1} ; UV–vis (CH_2Cl_2) λ_{max} (log ϵ) 356 (4.94), 460 (5.16), 539 (4.80), 719 (4.49) nm; HRMS m/z calcd for $\text{C}_{90}\text{H}_{90}$ + H 1171.7121, found 1171.7141. Limited solubility of **21** and **22** in organic solvents precluded ^{13}C NMR spectroscopy.

4,5,9,10-Tetrabromo-2,7-di-tert-butyl-trans-10b,10c-dimethyl-10b,10c-dihdropyrene (30). A solution of Br_2 (2.05 g, 12.8 mmol) in CCl_4 (160 mL) was added dropwise to a solution of dihydropyrene **11**³⁵ (1.10 g, 3.20 mmol) in CCl_4 (200 mL) at 0 °C over 1 h. The mixture was stirred for an additional 1 h and then poured into ice–water. The mixture was extracted with CH_2Cl_2 (300 mL), and the organic layer was washed with water, dried (MgSO_4), and concentrated. Recrystallization (hexane) yielded **30** (2.01 g, 95%) as green crystals: mp 227–229 °C (lit.³⁵ mp 228–230 °C).

Bis[14]polyynes–DDP 31. Tetrabromo **30** (73 mg, 0.11 mmol), 1-ethynyl-2-(triisopropylsilyl)ethynylbenzene^{8b} (244 mg, 0.86 mmol), $\text{PdCl}_2(\text{PPh}_3)_2$ (6 mg, 0.009 mmol), $\text{Pd}(\text{PPh}_3)_4$ (4 mg, 0.004 mmol), CuI (10 mg, 0.053 mmol), Et_3N (1.5 mL), and DMF (1.5 mL) were reacted using general procedure A. Purification by preparative TLC (7:1 hexanes/ CH_2Cl_2) gave **31** (86 mg, 53%) as a brown powder: mp 271.0–272.4 °C; ^1H NMR (CDCl_3) δ 9.07 (s, 4H), 7.73–7.70 (m, 4H), 7.59–7.56 (m, 4H), 7.34–7.25 (m, 8H), 1.66 (s, 18H), 0.94 (s, 84H), –3.39 (s, 6H); IR (neat) ν 3061, 2924, 2864, 2155, 1465 cm^{-1} ; MS (FAB) m/z (rel intens) 1466 (42, M^+). Limited solubility of **31** in organic solvents precluded ^{13}C NMR spectroscopy.

Bis[14]DBA–DDP 3. Polyynes **31** (200 mg, 0.14 mmol) was dissolved in THF (10 mL) and MeOH (1 mL) and then treated with Bu_4NF (2.0 mL, 1.0 M in THF) using general procedure B. The deprotected polyynes were dissolved in pyridine (5 mL) and THF (3 mL) and then added slowly over 8 h to a slurry of CuCl (166 mg, 1.68 mmol) and pyridine (10 mL) at rt under house air. After 48 h, the solvent was evaporated and the residue was redissolved in CH_2Cl_2 . The slurry was filtered through silica gel and the filtrate concentrated to give a dark semisolid. Purification by preparative TLC (2:1 hexanes/ CH_2Cl_2) gave **3** (22 mg, 16%) as a red-brown powder: mp > 350 °C; ^1H NMR (CDCl_3) δ 9.65 (s, 4H), 8.36 (d, J = 6.9 Hz, 4H), 7.70–7.65 (m, 8H), 7.55–7.50 (m, 4H), 1.95 (s, 18H), –3.33 (s, 6H); IR (KBr) ν 3059, 2962, 2924, 2865, 2220, 2161, 1474, 752 cm^{-1} ; UV–vis (CH_2Cl_2) λ_{max} (log ϵ) 277 (4.64), 300 (4.66), 320 (4.64), 440 (4.67), 470 (4.87), 540 (4.20), 616 (3.42), 679 (3.43), 758 (4.03) nm; MS (MALDI-TOF) m/z (rel intens) 837.90 (52, M^+). Limited solubility of **3** in organic solvents precluded ^{13}C NMR spectroscopy.

4,5,9,10-Tetrakis[dimethyl(1,1,2-trimethylpropyl)silyl-ethynyl]-2,7-di-tert-butyl-trans-10b,10c-dimethyl-10b,10c-dihydropyrene (33). Tetrabromo **30** (350 mg, 0.530 mmol), dimethylethynyl(1,1,2-trimethylpropyl)silane (897 mg, 5.33 mmol), PdCl₂(PPh₃)₂ (25 mg, 0.036 mmol), Pd(PPh₃)₄ (21 mg, 0.018 mmol), CuI (10 mg, 0.053 mmol), Et₃N (3.5 mL), and DMF (3.5 mL) were reacted using general procedure A. Purification by preparative TLC (9:1 hexanes/CH₂Cl₂) gave **33** (177 mg, 33%) as a green-black powder: mp > 350 °C; ¹H NMR (CDCl₃) δ 9.02 (s, 4H), 1.91 (septet, *J* = 6.9 Hz, 4 H), 1.67 (s, 18H), 1.15 (s, 24H), 1.04 (d, *J* = 6.9 Hz, 24 H), 0.45 (s, 12H), 0.43 (s, 12H), -3.53 (s, 6H); ¹³C NMR (CDCl₃) δ 149.70, 139.07, 122.22, 117.99, 104.49, 103.43, 36.49, 34.59, 31.75, 30.62, 23.63, 21.06, 18.86, 15.72, -1.81; IR (KBr) ν 2959, 2925, 2864, 2136, 1249, 821, 772 cm⁻¹; UV-vis (CH₂Cl₂) λ_{max} (log ε) 265 (4.43), 288 (4.14), 295 (4.12), 307 (4.18), 314 (4.13), 327 (4.16), 405 (4.13), 432 (4.22), 504 (3.21), 728 (2.84) nm; HRMS *m/z* calcd for C₆₆H₁₀₅Si₄ 1009.7293, found 1009.7274.

Bis[18]polyne-DDP 34. Tetrayne **33** (50 mg, 0.05 mmol) was dissolved in THF (2 mL) and MeOH (0.1 mL) and then treated with Bu₄NF (0.5 mL, 1.0 M in THF) using general procedure B. After workup, the desilylated tetrayne (~19 mg, 0.05 mmol) dissolved in THF (2 mL) and DMSO (2 mL) was added to an argon-degassed mixture of 1-bromoethynyl-2-(triisopropylsilyl)ethynylbenzene^{8b} (72 mg, 0.2 mmol), Pd(dba)₂ (3.5 mg, 0.006 mmol), CuI (1.0 mg, 0.005 mmol), LiI (7.5 mg, 0.04 mmol), and DMSO (2 mL) using the procedure of Vasella.²⁴ The reactants were stirred for 5 min at rt, and then 1,2,2,6,6-pentamethylpiperidine (87 mg, 0.56 mmol) was added. After 48 h, Et₂O (35 mL) and 10% aq NH₄Cl solution (10 mL) were added. The organic layer was washed with H₂O, dried (MgSO₄), filtered, and concentrated. Purification by preparative TLC (4:1 petroleum ether/CH₂Cl₂) gave **34** (62 mg, 80%) as a black semisolid: ¹H NMR (CDCl₃) δ 9.02 (s, 4H), 7.64–7.61 (m, 4H), 7.55–7.52 (m, 4H), 7.35–7.28 (m, 8H), 1.73 (s, 18H), 1.14 (s, 84H), -3.39 (s, 6H); ¹³C NMR (CDCl₃) δ 151.47, 140.52, 133.07, 132.43, 128.57, 127.92, 127.04, 125.15, 122.64, 117.65, 104.67, 96.18, 84.08, 83.45, 81.09, 78.55, 36.59, 31.73, 18.71, 16.15, 11.29; IR (KBr) ν 3060, 2943, 2942, 2864, 2202, 2156, 1462, 756 cm⁻¹; MS (FAB) *m/z* (rel intens) 933.3 (36, M⁺), 918.3 (M⁺ - Me), 903.3 (M⁺ - 2Me), 176 (100).

Bis[18]DBA-DDP 32. Polyne **34** (45 mg, 0.04 mmol) was dissolved in THF (5 mL) and MeOH (0.5 mL) and then treated with Bu₄NF (1.0 mL, 1.0 M in THF) using general procedure B. After workup, the deprotected polyne was dissolved in THF (6 mL) and added slowly over 8 h to a slurry of Cu(OAc)₂ (213 mg, 1.1 mmol) in THF (3 mL) and pyridine (9 mL) at rt under house air. After 48 h, the solvent was evaporated and the residue redissolved in CH₂Cl₂. The solution was filtered through silica gel and the filtrate concentrated. Purification of the dark residue by column chromatography (4:1 petroleum ether/CH₂Cl₂/THF) gave **32** (13 mg, 47%) as a dark violet-black powder: mp > 350 °C; ¹H NMR (CDCl₃) δ 9.18 (s, 4H), 7.84–7.81 (m, 4H), 7.71–7.68 (m, 4H), 7.49–7.41 (m, 8H), 1.84 (s, 18H), -3.49 (s, 6H); IR (KBr) ν 3058, 2958, 2926, 2904, 2867, 2189, 2133, 752 cm⁻¹; UV-vis (CH₂Cl₂) λ_{max} (log ε) 293 (4.85), 305 (4.87), 326 (4.87), 455 (5.03), 476 (5.22), 544 (4.67), 624 (3.82), 693 (3.82), 767 (4.60) nm; MS (FAB) *m/z* (rel intens) 932 (15, M⁺). Limited solubility of **32** in organic solvents precluded ¹³C NMR spectroscopy.

4,5,9,10-Tetra(phenylethynyl)-2,7-di-tert-butyl-trans-10b,10c-dimethyl-10b,10c-dihydropyrene (35). Tetrayne **33** (42 mg, 0.042 mmol) was dissolved in THF (8 mL) and MeOH (0.5 mL) and treated with Bu₄NF (0.5 mL, 1.0 M in THF) using general procedure B. After workup, the crude product was combined with iodobenzene (0.094 mL, 0.84 mmol), PdCl₂(PPh₃)₂ (2 mg, 0.003 mmol), Pd(PPh₃)₄ (3 mg, 0.003 mmol), CuI (2 mg, 0.012 mmol), and Et₃N (10 mL). The mixture was degassed by three successive freeze-pump-thaw cycles, flushed with N₂, and stirred at 60 °C for 48 h. After cooling, the solvent was evaporated and the residue was redissolved in Et₂O. The solution was vacuum filtered through Celite and silica gel and then concentrated. Purification by

preparative TLC (9:1 hexanes/CH₂Cl₂) gave **35** (27 mg, 87%) as a deep red powder: mp 241.0–243.1 °C; ¹H NMR (CDCl₃) δ 9.18 (s, 4H), 7.82 (d, *J* = 7.2 Hz, 8H), 7.50–7.40 (m, 12H), 1.79 (s, 18H), -3.32 (s, 6H); ¹³C NMR (CDCl₃) δ 138.51, 131.60, 128.57, 128.29, 124.08, 122.07, 117.98, 99.18, 88.97, 36.53, 31.83, 16.06; IR (KBr) ν 3081, 2961, 2920, 2855, 1493, 759, 749 cm⁻¹; UV-vis (CH₂Cl₂) λ_{max} (log ε) 292 (4.30), 423 (4.79), 449 (4.91), 515 (4.19), 601 (2.95), 670 (2.99), 740 (3.92) nm; HRMS *m/z* calcd for C₅₈H₄₈ 744.3756, found 744.3769.

trans-4,5-Dibromo-2,7-di-tert-butyl-12c,12d-dihydro-12c,12d-dimethylbenzo[el]pyrene (36). A solution of benzo-DDP **27**¹⁷ (285 mg, 0.72 mmol) in dry CH₂Cl₂ (200 mL) was prepared under argon in the dark and cooled in an ice bath. NBS (257 mg, 1.44 mmol) in dry DMF (40 mL) was added slowly with stirring. The reaction was allowed to warm to 20 °C and stirred for 2 h. The mixture was poured into hexanes and washed with water. The organic phase was dried (MgSO₄) and concentrated. The residue was purified from fluorescent pyrenes by chromatography over silica gel (9:1 hexanes/CH₂Cl₂) deactivated with 5% water. Repeating the chromatography three additional times yielded **36** (191 mg, 48%) as intense purple crystals from cyclohexane: mp 187–189 °C dec; ¹H NMR (CDCl₃) δ 8.69–8.64 (AA'XX'm, 2H), 8.21 (d, *J* = 1.3 Hz, 2H), 7.73 (d, *J* = 1.3 Hz, 2H), 7.65–7.60 (AA'XX'm, 2H), 1.49 (s, 18H), -1.30 (s, 6H); ¹³C NMR (CDCl₃) δ 148.67, 136.16, 135.71, 129.15, 126.67, 124.69, 120.15, 117.51, 117.04, 39.13, 35.87, 30.37, 17.34; IR (KBr) ν 866, 754, 610 cm⁻¹; MS (CI) *m/z* 551 (M⁺ + H, correct isotope pattern). Anal. Calcd for C₃₀H₃₂Br₂: C, 65.23; H, 5.84. Found: C, 65.33; H, 5.89.

Benzo-DDP-[14]DBA Polyne 37. Dibromo-DDP **36** (40 mg, 0.072 mmol), 1-ethynyl-2-(triisopropylsilyl)ethynylbenzene^{8b} (51 mg, 0.18 mmol), PdCl₂(PPh₃)₂ (5.2 mg, 0.0074 mmol), Pd(PPh₃)₄ (4.3 mg, 0.0037 mmol), CuI (3 mg, 0.016 mmol), Et₃N (1 mL), and DMF (3 mL) were reacted using general procedure A. Column chromatography (9:1 hexanes/CH₂Cl₂) provided **37** (53 mg, 77%) as a dark red oil: ¹H NMR (CDCl₃) δ 8.70 (br s, 2H), 8.23 (s, 2H), 7.99 (s, 2H), 7.64–7.61 (m, 2H), 7.60–7.57 (m, 2H), 7.53–7.50 (m, 2H), 7.24–7.16 (m, 4H), 1.94 (s, 18H), 1.02 (s, 21H), 1.01 (s, 21H), -1.24 (s, 6H); ¹³C NMR (CDCl₃) δ 132.72, 129.28, 127.78, 127.23, 126.95, 126.32, 125.43, 124.54, 118.80 (br), 117.67 (br), 114.90, 105.91, 95.52 (br), 94.67, 36.36, 30.38, 18.71, 18.12, 11.29; IR (neat) ν 3061, 2960, 2864, 2197, 2955 cm⁻¹; UV-vis (CH₂Cl₂) λ_{max} (log ε) 239 (5.01), 271 (5.13), 362 (4.43), 401 (4.63), 420 (4.75), 527 (3.76) nm; HRMS *m/z* calcd for C₆₈H₈₃Si₂ 955.6033, found 955.6058.

Benzo-DDP-[14]DBA 4. Polyne **37** (45 mg, 0.047 mmol) was treated with Bu₄NF (1 mL, 1.0 M in THF) in MeOH (0.7 mL) and THF (20 mL) using general procedure B. After workup, the desilylated product was dissolved in THF (9 mL) and added over 8 h to a slurry of CuCl (400 mg, 4.0 mmol), MeOH (5 mL), and pyridine (15 mL) under air at rt. After the solution was stirred for an additional 48 h, the volatiles were evaporated and the residue was dissolved in CH₂Cl₂ and vacuum filtered through silica gel. Purification by preparative TLC (4:1 petroleum ether/CH₂Cl₂) gave **4** (27 mg, 90%) as a dark purple powder: mp 197 °C dec; ¹H NMR (CDCl₃) δ 8.77–8.74 (m, 2H), 8.36 (s, 2H), 8.31 (s, 2H), 7.97 (d, *J* = 7.6 Hz, 2H), 7.70–7.67 (m, 2H), 7.47–7.40 (m, 4H), 7.31 (t, *J* = 7.6 Hz, 2H), 1.62 (s, 18H), -1.32 (s, 6H); ¹³C NMR (CDCl₃) δ 148.84, 144.27, 137.82, 132.93, 131.54, 129.50, 129.42, 129.05, 127.64, 126.95, 124.89, 122.69, 119.00, 117.95, 113.03, 98.09, 94.04, 87.18, 80.66, 37.02, 30.99, 18.09; IR (neat) ν 3060, 2961, 2924, 2864, 2165 cm⁻¹; UV-vis (CH₂Cl₂) λ_{max} (log ε) 230 (4.94), 298 (4.74), 319 (4.76), 439 (4.79), 550 (3.83) nm; HRMS *m/z* calcd for C₅₀H₄₀ 640.3130, found 640.3118.

Benzo-CPD-[14]DBA 38. To an NMR tube were added **4** (8 mg, 0.012 mmol) and CDCl₃ (1.0 mL). The solution was irradiated in front of an overhead projector for 5 min, during which the dark green-brown solution turned deep red: ¹H NMR (CDCl₃) δ 7.92–7.89 (m, 2H), 7.78–7.71 (m, 4H), 7.67 (d, *J* = 1.8 Hz, 2H), 7.54–7.51 (m, 4H), 7.46–7.44 (m, 2H), 6.97 (d, *J* = 1.8 Hz, 2H), 1.34 (s, 6H), 1.33 (s, 18H); ¹³C NMR (CDCl₃) δ 150.84, 144.18, 140.28, 139.24, 138.49, 133.21,

129.27, 129.71, 129.49, 129.37, 128.90, 128.86, 128.64, 128.28, 126.08, 122.47, 97.88, 96.97, 86.80, 80.77, 34.59, 31.60, 19.08; UV–vis (CH₂Cl₂) λ_{max} (log ϵ) 230 (4.96), 307 (4.78), 320 (4.80), 418 (4.41), 437 (4.45).

Acknowledgment. We thank the Petroleum Research Fund (M.M.H.), administered by the American Chemical Society, the Natural Sciences and Engineering Research Council of Canada (R.H.M.), the University of Idaho for a Seed Grant (R.V.W.), and The Camille and Henry Dreyfus Foundation (Teacher-Scholar Award 1998–2003 to M.M.H.) for financial support.

Supporting Information Available: Calculated bond lengths and bond alternations for the DDP nucleus of **1**, **2**, and **26** (Table S1), calculated bond lengths for the ODA nucleus of **1**, **2**, **14**, **25**, and **26** (Table S2), calculated and experimental ¹H and ¹³C NMR chemical shifts for **1**, **2**, **14**, **25**, and **26** (Tables S3 and S4), Cartesian coordinates of **1**, **2**, **14**, **25**, and **26** optimized using the B3LYP/6-31G* method, and ¹³C NMR spectra for compounds **1**, **4**, **9–10**, **13**, **16**, **18**, **20**, **33–35**, and **37**. This material is available free of charge via the Internet at <http://pubs.acs.org>.

JO020462Q